Biogeochemistry (2014) 118:413–442
DOI 10.1007/s10533-013-9941-2

The dynamics of calcium and magnesium inputs by throughfall in a forest ecosystem on base poor soil are very slow and conservative: evidence from an isotopic tracing experiment (^{26}Mg and ^{44}Ca)

Gregory van der Heijden · Arnaud Legout · Benoît Pollier · Jacques Ranger · Etienne Dambrine

Received: 19 September 2013 / Accepted: 17 December 2013 / Published online: 7 January 2014

Abstract Using nutrient budgets, it has been proven that atmospheric deposition of Mg and Ca sustains the fertility of forest ecosystems on base-poor soils. However the fate of this nutrient input within the ecosystem was presently unknown. Our hypothesis is that the biological cycling of these nutrients is very rapid and conservative to prevent further Mg and Ca losses most especially in ecosystems on base-poor soils. Stable isotopes of magnesium and calcium (^{26}Mg and ^{44}Ca) were used to trace the dynamics of throughfall Mg and Ca in the forest soil of a 35-year-old beech stand. The aim of the present study was to (1) understand the processes and the velocity of the incorporation of tracers in the biogeochemical cycles and (2) compute Mg and Ca budgets for the ecosystem by isotope dilution. Rainfall Mg and Ca were strongly and rapidly retained mainly by ion exchange in the thin OL litter-layer. However, Ca was much more strongly retained in the litter-layer than Mg. As a result, 2 years after the application of tracers (2012), 92 % of ^{26}Mg and 67 % of ^{44}Ca was released and transferred to the soil or taken up by trees. The vertical transfer of Mg was very slow only 15 % of ^{26}Mg was found below 15 cm depth in 2012. Ca was slower than ^{26}Mg only 9 % of ^{44}Ca was found below 5 cm depth. Although matrix flow was the main vertical transfer process of Ca and Mg, preferential transfer in macropores occurred. Overall, Mg was more rapidly leached through the soil profile than Ca because the soil CEC was mainly composed of organic charges which affinity for Ca is much higher than for Mg. 27 % of ^{26}Mg and 20 % of ^{44}Ca was found in tree biomass and total tracer recovery was close to 100 %. These results suggest that no tracers were lost to drainage over the 2 years. Finally, applying the isotopic dilution theory to the whole-ecosystem enabled us to estimate Mg and Ca budgets -0.9 kg ha^{-1} year^{-1} for Mg, which was close to computed input–output budgets -0.8 and 0 kg ha^{-1} year^{-1} for Ca, which was very different from input–output budgets (-3.1 kg ha^{-1} year^{-1}). Our results suggest that a Ca source is underestimated or not taken into account. Over all, organic matter of the litter-layer and in the soil profile played an essential role in the retention of

Responsible Editor: Robert Cookon.

G. van der Heijden (✉) · A. Legout · B. Pollier · J. Ranger
Unité Biogéochimie des Ecosystèmes Forestiers, INRA de Nancy, Route d'Amance, 54280 Champenoux, France
e-mail: gregory.vanderheijden@nancy.inra.fr

A. Legout
e-mail: legout@nancy.inra.fr

B. Pollier
e-mail: pollier@nancy.inra.fr

J. Ranger
e-mail: ranger@nancy.inra.fr

E. Dambrine
INRA-Université de Savoie, UMR Carrtel, 73376 Le Bourget du Lac, France
e-mail: dambrine@nancy.inra.fr

throughfall Mg and Ca and their cycling within the forest ecosystem.

Keywords Forest · Isotope tracer · Calcium · Magnesium · Soil fertility · Reactive transport

Introduction

Calcium and magnesium are two essential elements to forest soil fertility. Their amount on the cation exchange capacity directly influences soil base saturation and pH. As divalent cations, they participate in the binding of negatively charged particles such as clays and organic compounds and therefore stabilize soil structure and aggregates. Calcium is also essential for the biological activity of many soil organisms, such as earthworms, which influence considerably litter decomposition (Edwards and Bohlen 1996). Finally calcium and magnesium are essential for plant nutrition (Marschner 1995).

Most forest soils are acid and base poor. Stores of bioavailable Ca and Mg originate from inputs by atmospheric deposition and mineral weathering and vary in relation to leaching and biomass immobilization. In numerous situations, nutrient budget approaches have questioned the sustainability of plant available Mg and Ca pools. Ongoing Ca and Mg depletion in soils, either related to decreasing atmospheric deposition rates (e.g. Jonard et al. 2012; van der Heijden et al. 2011) or to increased leaching (Bailey et al. 2005) or biomass immobilization (Johnson et al. 2008) was observed in many ecosystems throughout the world. In recent years, the demand for bio-energy has strongly increased supporting short rotation silviculture and whole-tree harvesting (Ericsson 2004; Puech 2009). The sustainability of forest ecosystems on base-poor soils is uncertain in such a context.

Paradoxally, in many forest ecosystems, low available Mg and Ca pools and Mg and Ca depletion have not been reflected in tree growth and health. In many cases, computed input–output nutrient budgets were in disagreement with measured soil nutrient pool size change over time. For example, in a silver fir stand in the Vosges Mountains (France), input–output budgets computed over a 13-year period predicted Mg and Ca depletion (on average -0.8 kg ha^{-1} year^{-1} Mg and -1.9 kg ha^{-1} year^{-1} Ca) while soil sampling showed that the exchangeable Mg and Ca pools in the 0–70 cm mineral soil had remained constant (van der Heijden et al. 2011). Hazlett et al. (2011) also observed no change in exchangeable Mg and Ca pools over a 17–19-year period in the soil of the Turkey Lakes catchment in Canada although input–output budgets predicted Mg and Ca depletion (-0.5 kg ha^{-1} year^{-1} Mg and -32 kg ha^{-1} year^{-1} Ca). Input–output budgets computed by Johnson et al. (1982) in an oak stand after clear-cut predicted Ca depletion but were contradicted by soil resampling 15 years after the clear-cut: soil exchangeable Ca pools had remained constant (Johnson and Todd 1998). In other cases, no forest decline symptoms were observed although available Mg and Ca pools in the soils were very low (van der Heijden et al. 2013c).

To explain such discrepancies, many authors have suggested that the nutrient fluxes measured for the purpose of input–output budgets may be poorly estimated. The difficulty of estimating atmospheric dry deposition has been discussed by Staelens et al. (2008) and recently Lequy et al. (2012) showed that aeolian dry dust deposition (not previously taken into account) is also a nutrient input to forest ecosystems. Estimating mineral weathering is also known to be a large source of error. For example, Klaminder et al. (2011) showed that the relative standard error around the mean Ca and K weathering flux (mean of seven different approaches to estimate weathering fluxes in the Svartberget–Kryclan catchment in Sweden) was, respectively, 105 and 97 %. Quantifying the biological component of the weathering flux is also difficult although such processes have been shown to be very important in plant nutrition (Arocena et al. 2012; Calvaruso et al. 2006; Turpault et al. 2009). Yanai et al. (2005) also showed that the weathering of apatite minerals in the soils, which are often not taken into account in weathering budgets, may mitigate Ca depletion in the north-eastern states of USA. Finally, it has also been shown that in forest ecosystems on base-poor soils, biological cycling represents a greater pool of nutrients than mineral soil pools (van der Heijden et al. 2013c). Overall these discrepancies show the need to more precisely define what nutrient pools are available for plant uptake and how nutrients transfer in between the different ecosystem compartments. They also show the limits of conventional approaches to study nutrient pools and fluxes.

We hypothesize that in forest ecosystems where Mg and Ca inputs, whether through atmospheric deposition or mineral weathering, are low, the Mg and Ca plant-available pools are sustained over time by a rapid and conservative biological cycling of these nutrients. To properly test our hypothesis, the development of new methods was necessary.

The development of mass spectrometry instruments has enabled to use stable isotopes (such as ^{15}N, ^{18}O, ^{2}H, ^{13}C and more recently ^{26}Mg and ^{44}Ca), as tracers to gain insight in nutrient cycling in forest ecosystems. The natural variation of Mg and Ca stable isotope ratios has enabled to trace processes such as root uptake, allocation and translocation (Bolou-Bi et al. 2010; Cobert et al. 2011; Hindshaw et al. 2012). However, because the Mg and Ca isotope ratios of bulk deposition and Ca- or Mg-bearing minerals often overlap and given the precision of measurements, natural isotope variations enable to trace sources at specific sites only (Bolou-Bi et al. 2012; Holmden and Bélanger 2010). Moreover, fluxes are generally computed assuming steady state. The isotopic labeling technique with ^{26}Mg and ^{44}Ca enriched material is a complementary approach and enables to trace fluxes between ecosystem compartments by artificially changing the isotopic composition of a given pool (Augusto et al. 2011; Kuhn et al. 2000; Midwood et al. 2000; Weatherall et al. 2006).

In order to test our hypothesis, an in situ ecosystem-scale multi-isotopic (^{2}H, ^{15}N, ^{26}Mg and ^{44}Ca) tracing experiment was carried out in April 2010 in a 35-year-old beech plot at the Breuil-Chenue experimental site. This site was selected for the multi-isotopic tracing experiment (described below) for the following reasons: (i) Conventional and isotopic approaches to study nutrient cycling may be compared at this site. Indeed, the site has been intensively monitored since 2002 and nutrient fluxes and input–output budgets have been computed (van der Heijden et al. 2013c). (ii) Soil Mg and Ca pools in the ecosystem were very low: the application of a small amount of ^{26}Mg and ^{44}Ca enriched material may strongly label theses pools. (iii) Nutrient pools in the soil at this site are very low. Indeed, exchangeable Mg and Ca pools were respectively 33 kg ha^{-1} Mg and 61 kg ha^{-1} Ca in 2001 and nutrient budgets for this stand over 2003–2008 predicted Mg and Ca depletion (-0.8 kg ha^{-1} $year^{-1}$ Mg and -3.1 kg ha^{-1} $year^{-1}$ Ca). However, no forest decline symptoms (yellowing or loss of leaves, etc.) were observed. Tree growth and health was apparently not impaired.

This paper focuses on the fate of ^{26}Mg and ^{44}Ca in the ecosystem. Previous papers have reported results from this experiment:

Water fluxes in the soil were studied in van der Heijden et al. (2013b). Modeling and ^{2}H water tracing results evidenced the occurrence of preferential water flow in the soil profile.

Nutrient pools and fluxes and input–output budgets computed with "conventional" approaches were reported in van der Heijden et al. (2013c). Soil exchangeable pools were measured in 1976 and again in 2001. The comparison of both sampling dates suggested that Mg was depleted from the soil (-5 kg ha^{-1} $year^{-1}$) while Ca pools remained constant. Nutrient fluxes were monitored over the 2003–2008 period and input–output budgets suggested both Mg and Ca depletion -0.8 and -3.1 kg ha^{-1} $year^{-1}$ respectively.

Isotope ratio analysis with ICP-MS methods were reported in van der Heijden et al. (2013a). Preliminary results reported in this article showed that the litter-layer plays an important role in retaining Mg and Ca inputs from rainfall/throughfall, and that a both rapid and slow vertical transfer of tracers occurred in the soil profile.

The aim of the present study was to (1) understand the processes and the velocity of the incorporation of tracers in the biogeochemical cycles and (2) compute Mg and Ca budgets for the ecosystem by isotope dilution. In order to do so, we first measured the tracer concentrations in the litter-layer (bulk litter and exchangeable), the mineral soil (microbial biomass and exchangeable), soil solution and above-ground biomass 2 years following the application of tracers to study Mg and Ca dynamics in the ecosystem. Then we estimated Mg and Ca pool sizes in the different ecosystem compartments in 2012 by applying the isotopic dilution theory and compared this to former measurements.

Materials and methods

Study site

The experimental site of Breuil-Chenue forest (hereafter named Breuil-Chenue site) is located in the

Table 1 Breuil-Chenue experimental site soil description from 16 sampled profiles in 2001, data from van der Heijden et al. (2013a)

Horizon	Depth (cm)	Bulk density ($\phi < 2$ mm)	Soil texture			C (g kg^{-1})	C/N	Soil cationic exchange capacity				
			Sand (%)	Silt (%)	Clay (%)			ECEC ($cmol_c$ kg^{-1})	Organic CEC (%)	BS (%)	Mg ($cmol_c$ kg^{-1})	Ca ($cmol_c$ kg^{-1})
A1/E	0–5	0.50	57.6	21.8	20.6	72.6	18.0	8.66	74	19.4	0.23	0.54
A1–A1/Bp	5–10	0.64	60.2	21.5	18.4	46.1	18.1	7.23	63	10.9	0.13	0.15
Sal 1	10–15	0.67	58.0	23.6	18.4	34.2	18.1	5.43	57	7.9	0.08	0.07
Sal 2	15–25	0.89	60.0	24.1	16.0	23.3	17.9	4.08	51	5.8	0.04	0.02
Sal 2	25–40	0.90	57.8	24.7	17.5	14.0	17.1	3.13	38	7.4	0.03	0.02
Sal 3	40–55	1.08	55.7	25.8	18.5	–	–	3.11	–	8.1	0.02	0.01
II Sal 4	55–70	1.05	57.3	25.3	17.5	–	–	3.32	–	8.1	0.03	0.02

Bulk density is given for the soil particules smaller than 2 mm diameter (mass of soil particles smaller than 2 mm/total volume of soil). Organic CEC is the relative contribution of soil organic matter to soil total ECEC (expressed in %) and was estimate with Eq. (1) (Table 2). Base saturation (BS) is expressed in percentage of the effective cationic exchange capacity (ECEC)

Morvan Mountains, Burgundy, France (latitude 47°18′10″, longitude 4°4′44″). The elevation is 640 m, the annual rainfall 1,180 mm, the mean annual potential evapo-transpiration (PET) 750 mm and the mean annual temperature 9 °C (computed over the period 2006–2010). The soil is a sandy Alocrisol (Alumic Cambisol; WRB FAO) displaying micro-podzolisation features in the upper mineral horizon (Ranger et al. 2004). The soil parent material is granite, containing 23.5 % quartz, 44 % K-feldspar, 28.5 % plagioclase, 1.6 % biotite and 1.6 % muscovite (Mareschal 2008). The experimental site is situated on a flat hilltop. The landscape is drained by a stream the source of which is situated ca. 500 m from the site. In 1975, part of the native forest (coppice with standards) located on a homogeneous soil type was clear-cut, heavy swathing was carried out. Effectively, all brash and the humus layer were removed from the plot. Plots (approximately 35 × 35 m^2) were planted with different species in 1976.

The present study focused on the beech plot (*Fagus silvatica* L.). The humus type in this plot was described in 2003 as a mesomull (Brethes et al. 1995): the OL-layer was 0.5–1 cm thick, the OF-layer was very thin and discontinuous and no OH-layer was observed (Moukoumi 2006). The humus layer (hereafter referred to as the litter-layer) represented 22,000 kg ha^{-1} of dry matter, 12 kg ha^{-1} of Mg and 54 kg ha^{-1} of Ca. Soil chemical properties were measured from 16 soil profiles (0–70 cm depth) collected in 2001. A description of soil properties is given in Table 1. The proportion of organic CEC in total soil CEC was estimated by fitting the following equations to the soil analysis data:

$$\mathrm{CEC_{total}} = a + b \times \mathrm{Carbon}(\%) + c \times \mathrm{Clay}(\%) \quad (1)$$

where $\mathrm{CEC_{total}}$ is the total measured cationic exchange capacity ($cmol_c$ kg^{-1}), Carbon(%) the soil total

Table 2 Statistics for the fitted parameters of Eq. (1) predicting fine earth total CEC from soil carbon content (%) (*b*) and clay content (%) (*c*)

	Estimate	SE	Pr (>|t|)
a	–	–	NS
b	0.92191	0.075	<0.0001
c	0.12374	0.01818	<0.0001
			$R^2 = 0.9881$

Parameters were fitted with a linear regression model

carbon content (%), Clay(%) the soil clay content (%) and *a*, *b* and *c* the fitted parameters. The parameters (*a*, *b* and *c*) were assumed to be constant with depth and were fitted using a linear regression model (Table 2) (Evans 1982; Helling et al. 1964; Pratt 1961; Wilding and Rutledge 1966; Wright and Foss 1972; Yuan et al. 1967).

Nutrient pools (soil, litter and aboveground biomass) in 2001 and nutrient fluxes and input–output budgets were computed for the beech plot over the 2003–2008 period (Table 3). Methods were fully described in a previous paper (van der Heijden et al. 2013c). Briefly, the litter-layer pool was estimated from 16 samples collected in 2001. The aboveground biomass pool was estimated with allometric equations fitted to 14 trees sampled during a thinning in 2002. Atmospheric wet deposition was computed from bulk rainfall. Atmospheric dry deposition was estimated using the equations defined by Ulrich (1983). We assumed that no Na^+ canopy interaction and computed dry Na deposition as the difference between bulk rainfall and throughfall plus stemflow. Dry deposition of cations (Ca^{2+}, Mg^{2+}, K^+ and NH_4^+) was then computed using the Na dry deposition factor. We used the geochemical model PROFILE (Sverdrup and Warfvinge 1988) to calculate the mean annual input. Fine earth (soil particles smaller than 2 mm diameter) mineralogy (Mareschal 2008) was implemented in PROFILE and the mineral surface area was calibrated so as to reproduce Na concentrations in the soil solution. The leaching flux at 60 cm depth was estimated by multiplying the mean measured tension-cup lysimeter concentration with the modelled water drainage flux. The water drainage flux was modelled with BILJOU (Granier et al. 1999), a pool and flux model. The model was calibrated over 2002–2008 using daily soil water content data collected with TDR probes (van der Heijden et al. 2013b). Forest inventories were carried out yearly from 2002 to 2008 and allometric equations were applied to these inventories. Net uptake was computed from the difference of immobilised nutrients between two consecutive years.

Table 3 Mg and Ca pools in 2001, fluxes and input–output budgets computed over 2003–2008

	Mg (kg ha^{-1})		Ca (kg ha^{-1})	
Pools in 2001				
Aboveground biomass	25	(0.4)	148	(3.4)
Litter-layer (bulk)	12	(4.6)	55	(17.6)
Mineral soil 0–70 cm (exchangeable)	33	(8)	61	(28)
Inputs				
Atmospheric deposition	0.8	(0.2)	3.7	(1.5)
Weathering	0.5	–	0.2	–
Cycling				
Throughfall	0.8	(0.1)	3.0	(0.7)
Litterfall	1.6	(0.3)	10.4	(1.3)
Outputs				
Leaching 60 cm	0.9	(0.2)	1.4	(0.3)
Net uptake	1.2	(0.2)	5.6	(0.8)
Budget	−0.8	(0.3)	−3.1	(1.2)

Figures between brackets are estimated uncertainties: standard deviation of sample replicates for pools, annual fluxes over 2003–2008 for fluxes and budgets and iterations ($n = 14$) of a Monte-Carlo approach for aboveground biomass. Data from van der Heijden et al. (2013c)

Multi-isotopic tracing experiment design

Application of stable isotope tracers

A subplot of the beech plot (hereafter named tracing plot) was equipped in 2009 to carry out a tracing experiment on April 7, 2010. The plot covered 80 m^2. The tracing solution (350 mg L^{-1} Mg; 200 mg L^{-1} Ca) was made up by dissolving enriched ^{26}MgO (99.25 at.% ^{26}Mg) and $^{44}CaCO_3$ (96.45 at.% ^{44}Ca). 20 L of the tracing solution were sprayed on the ground of the tracing plot representing a 0.25 mm rainfall event. 16 mm of deionised water were sprayed on the tracing plot over a period of 8 h so as to simulate a natural rainfall event. The application of Mg and Ca isotope tracers represented an input of 0.96 kg ha^{-1} Mg and 0.53 kg ha^{-1} Ca thus representing of 124 and 14 % of annual inputs. The tracing plot was monitored during the 2 years after the application of tracers as detailed below. To avoid a second application of tracer from litterfall, at each fall, all litterfall was collected by setting nets around each tree. Litterfall was replaced by fresh litter collected in the second 35 year-old beech plot of the Breuil-Chenue site.

Isotope ratio notation

Mg has three stable isotopes (mass 24–26) and Ca has six (mass 40, 42, 43, 44, 46 and 48). Crustal abundance values for Mg and Ca isotopes as detailed in Hoefs (2009) are ^{24}Mg (78.99 %), ^{25}Mg (10 %), ^{26}Mg (11.01 %), ^{40}Ca (96.941 %), ^{42}Ca (0.647 %), ^{43}Ca (0.135 %), ^{44}Ca (2.086 %), ^{46}Ca (0.004 %) and ^{48}Ca (0.187 %). Measured isotopic compositions of samples are expressed with the absolute value of the isotope ratio (^{26}Mg/^{24}Mg and ^{44}Ca/^{40}Ca) or in permil deviations relative to the Mg and Ca reference ratios [DSM3 (Galy et al. 2003) and NIST SRM 915a respectively]:

$$\delta^{26/24}\mathrm{Mg} = \left\{ \left(^{26}\mathrm{Mg}/^{24}\mathrm{Mg}\right)_{\mathrm{sample}} \Big/ \left(^{26}\mathrm{Mg}/^{24}\mathrm{Mg}\right)_{\mathrm{DSM3}} - 1 \right\} \times 1000 \quad (2)$$

$$\delta^{44/40}\mathrm{Ca} = \left\{ \left(^{44}\mathrm{Ca}/^{40}\mathrm{Ca}\right)_{\mathrm{sample}} \Big/ \left(^{44}\mathrm{Ca}/^{40}\mathrm{Ca}\right)_{\mathrm{NIST915a}} - 1 \right\} \times 1000 \quad (3)$$

To account for ^{26}Mg and ^{44}Ca applied tracers in each ecosystem compartment, it is necessary to distinguish ^{26}Mg and ^{44}Ca present naturally in Mg and Ca pools from ^{26}Mg and ^{44}Ca present due to the application of the tracers. Excess ^{26}Mg and ^{44}Ca in samples was calculated assuming that natural isotopic composition (control isotopic composition) was 0 ‰ for both Mg and Ca:

$$\mathrm{excess}(^{y}X) = [X]_{\mathrm{sample}} \times \left(\%\ ^{y}X_{\mathrm{sample}} - \%\ ^{y}X_{\mathrm{nat}}\right) \quad (4)$$

where excess(^{y}X) is the excess of the tracer isotope (^{26}Mg or ^{44}Ca) due to the application of the tracer in the sample, $[X]_{\mathrm{sample}}$ the concentration or total amount of element (Mg or Ca) in the sample, $\%\ ^{y}X_{\mathrm{sample}}$ the atom percent of the tracer isotope (^{26}Mg or ^{44}Ca) in the sample and $\%\ ^{y}X_{\mathrm{nat}}$ the atom percent of the tracer isotope (^{26}Mg or ^{44}Ca) at natural abundance (assumed 0 ‰). Atom percent of the tracer isotopes are calculated as follows:

$$\%^{26}\mathrm{Mg} = \frac{^{26}\mathrm{Mg}/^{24}\mathrm{Mg}}{1 + {}^{25}\mathrm{Mg}/^{24}\mathrm{Mg} + {}^{26}\mathrm{Mg}/^{24}\mathrm{Mg}} \quad (5)$$

$$\%^{44}\mathrm{Ca} = \frac{^{44}\mathrm{Ca}/^{40}\mathrm{Ca}}{1 + {}^{42}\mathrm{Ca}/^{40}\mathrm{Ca} + {}^{43}\mathrm{Ca}/^{40}\mathrm{Ca} + {}^{44}\mathrm{Ca}/^{40}\mathrm{Ca} + {}^{46}\mathrm{Ca}/^{40}\mathrm{Ca} + {}^{48}\mathrm{Ca}/^{40}\mathrm{Ca}} \quad (6)$$

where ^{26}Mg/^{24}Mg and ^{44}Ca/^{40}Ca are the measured ratios in samples, ^{25}Mg/^{24}Mg, ^{42}Ca/^{40}Ca, ^{43}Ca/^{40}Ca, ^{46}Ca/^{40}Ca and ^{48}Ca/^{40}Ca were assumed to be constant and equal to terrestrial values: 0.1266 for ^{25}Mg/^{24}Mg, 6.677×10^{-3} for ^{42}Ca/^{40}Ca, 1.3926×10^{-3} for ^{43}Ca/^{40}Ca, 4.1262×10^{-5} for ^{46}Ca/^{40}Ca and 1.929×10^{-3} for ^{48}Ca/^{40}Ca (Hoefs 2009).

Monitoring ^{26}Mg and ^{44}Ca isotope tracers in the ecosystems

Monitoring ^{26}Mg and ^{44}Ca tracers in the litter and mineral soil layers

During the 2 years after the tracing experiment, soil profiles were sampled with a cylindrical corer (sampling dates are given in Table 4) to measure the Mg and Ca isotopic composition of the litter-layer, the soil exchangeable pools and microbial biomass. The litter-layer was collected directly above the sampled soil profiles. Litter-layer samples were oven-dried (65 °C), milled and Mg and Ca tracers in the litter-layer were analysed in two different ways: (i) Exchangeable Mg and Ca and (ii) total Mg and Ca in litter. Exchangeable Mg and Ca in the litter-layer were measured after an extraction: 5 g of milled litter sample were shacked with 50 mL of 1 mol L^{-1} ammonium acetate then filtered. Total Mg and Ca in litter was measured after the digestion of ca 200 mg with of milled litter sample in 5 mL of 50 % nitric acid.

Sampled soil profiles were divided into 5 cm-thick layers down to 60 cm depth. Exchangeable Mg and Ca were measured after two consecutive extractions: 7.5 g of field fresh soil was shacked with 50 mL of

Table 4 Summary of soil and litter sampling dates, number of replicates and depth sampled

Date	Cumulated matrix water flow (mm)	Replicates	Sampled depth (cm)	Litter-layer	Soil extractions
08/04/2010	17.8	4	15	Yes	
14/04/2010	18.7	8	15	Yes	Yes
04/05/2010	38.3	8	15	Yes	Yes
18/05/2010	63.9	8	15	Yes	Yes
15/06/2010	96.7	8	15	Yes	Yes
15/07/2010	115.9	8	30	Yes	Yes
10/08/2010	126.1	8	30	Yes	
08/09/2010	158	8	15	Yes	Yes
04/10/2010	174.6	8	30	Yes	
04/11/2010	217.4	8	30	Yes	Yes
03/01/2011	361.3	8	30	Yes	
22/02/2011	429.5	8	30	Yes	
22/03/2011	481	8	45	Yes	Yes
19/04/2011	496.5	8	45	Yes	
16/05/2011	502.1	8	45	Yes	
11/07/2011	525.1	8	45	Yes	
05/09/2011	567.8	4	60	Yes	Yes
30/11/2011	646	4	60	Yes	
21/03/2012	884.6	4	60	Yes	Yes

The cumulated matrix water flow (mm) at each sampling date is also given (van der Heijden et al. 2013b)

1 mol L^{-1} ammonium acetate for 1 h then centrifuged. The supernatant was collected after each extraction and mixed together before being filtered.

Soil microbial biomass ^{26}Mg and ^{44}Ca were measured using a chloroform fumigation extraction (CFE) procedure (Brookes et al. 1982, 1985; Lorenz et al. 2010; Saggar et al. 1981; Sparling and West 1988; Vance et al. 1987): 7.5 g of field-fresh soil was weighed in glass vials and fumigated with chloroform for 24 h. Unfumigated samples served as controls. Fumigated samples were extracted following the same protocol as CEC extractions (detailed above). Excess ^{26}Mg and ^{44}Ca was computed for both fumigated and unfumigated samples with Eqs. (3) and (4). Microbial Mg, Ca, ^{26}Mg and ^{44}Ca were calculated based on 35 °C oven-dry soil by subtracting unfumigated soil extractions from fumigated soil extractions. Fumigated extractions were carried out on soil samples in the 0–30 cm soil layer and for samples collected from April 2010 to March 2012. Differences between fumigated and unfumigated extractions for total element (Mg, Ca and K) and isotope tracers (^{26}Mg and ^{44}Ca) were tested with an ANOVA test. Tracer pools in each compartment were computed from the measured isotope enrichment in each compartment and the total element (Mg and Ca) pool size. For the latter, the Mg and Ca pool size in litter in 2001 was used: we assumed that the nutrients in the litter pool have not changed since 2001.

Monitoring ^{26}Mg and ^{44}Ca tracers in soil solution

Soil solutions were collected every 28 days with hand-made PEHD zero-tension lysimeters (ZTLs) placed between the litter-layer and the soil surface (hereafter referred to as 0 cm depth) and at 10 cm depth (3 replicates/depth), and with ceramic tension-cup lysimeters (TCL; Oikos Umweltanalytik GBR, Ceramic P80, porosity 45 µm, alumina-silica), with an applied pressure of 0.6 bars, at 15, 30 and 60 cm depth (four replicates/depth). Solutions were stored in 60 mL polypropylene bottles at 4 °C.

Immobilization of ^{26}Mg and ^{44}Ca in tree biomass

In February 2012, a light thinning was carried out in the tracing plot and five trees were cut to measure ^{26}Mg and ^{44}Ca total uptake during the 2 years after the tracing experiment. The trunk of each felled tree was

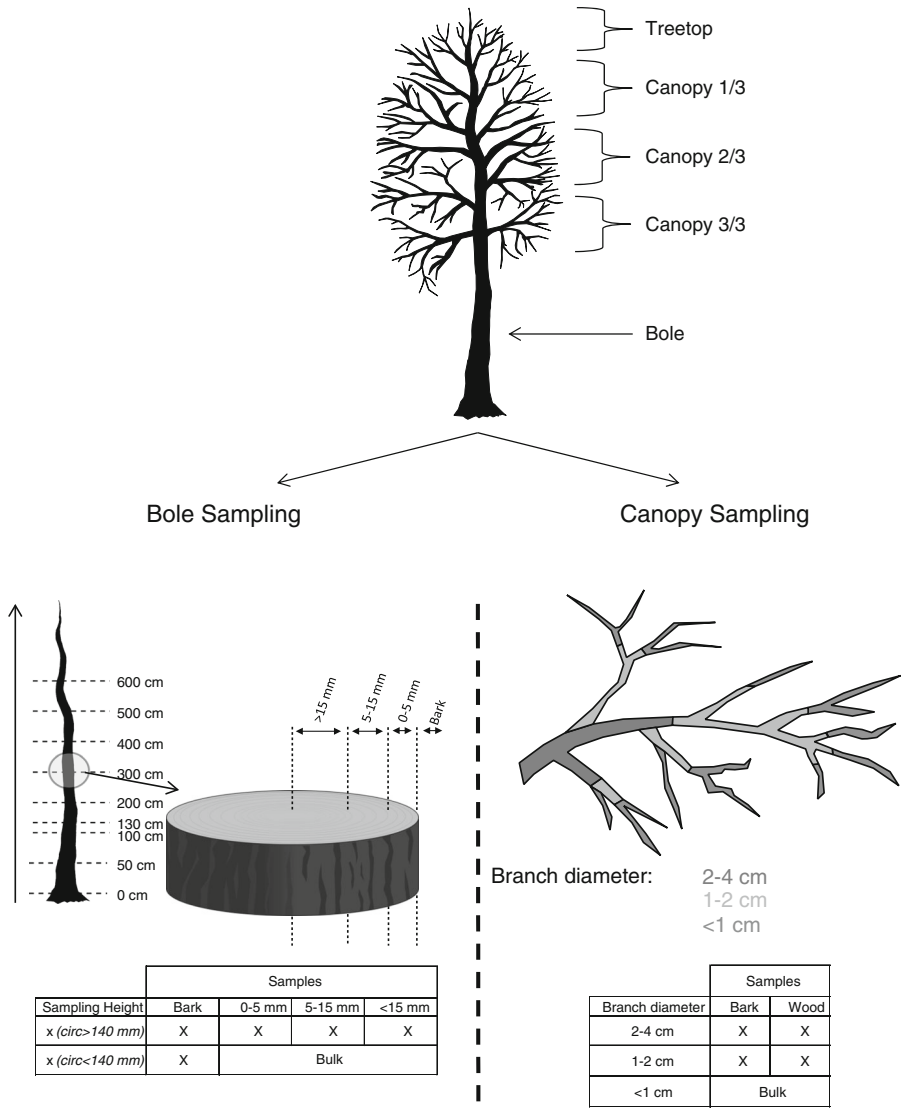

	Samples			
Sampling Height	Bark	0-5 mm	5-15 mm	<15 mm
x *(circ>140 mm)*	X	X	X	X
x *(circ<140 mm)*	X	Bulk		

	Samples	
Branch diameter	Bark	Wood
2-4 cm	X	X
1-2 cm	X	X
<1 cm	Bulk	

Fig. 1 Schematic description of the biomass sampling protocol to measure ^{26}Mg and ^{44}Ca immobilization in above-ground tree organs during the first 2 years after the application of tracers

cut into 1-m-long logs and each log was weighed (fresh weight), branches were separated according to their diameter and their height in the tree canopy (top, middle and bottom) and the fresh weight of each compartment was measured. A set of samples from each compartment were used to determine biomass water content: from the difference between fresh weight and 65 °C oven-dry weight. Another set of samples from each compartment (as detailed in Fig. 1) was oven-dried (65 °C), milled and digested in 50 % nitric acid to determine total element concentrations and Mg and Ca isotope ratios. Excess ^{26}Mg and ^{44}Ca was computed for each tree and each compartment with Eq. (4). One of the five trees showed die back symptoms (a significant amount of branches were dead) most probably because this tree was dominated by surrounding trees. ^{26}Mg and ^{44}Ca uptake for this particular tree was also low compared to the other sampled trees. We therefore considered this sampled tree as an outlier when fitting allometric equations.

Stumps were not removed during the thinning to avoid soil disturbances. Root tracer concentration and

biomass was thus not available. Root biomass in the Breuil-Chenue beech plot was estimated using biomass allometric equations fitted with root biomass data from a 25 year-old beech stand in Brittany, France (Legout 2008). Tracer immobilisation in the root biomass was estimated by multiplying predicted root biomass with measured tracer concentrations in the stump. Total immobilized tracer was then calculated for each tree and allometric equations using tree circumference at breast-height were fitted to the data.

Sample analysis methods

Ca and Mg concentrations in samples (soil solutions, soil CEC extractions, biomass digests) were measured by ICP-AES (Jobin–Yvon 180 ULTRACE) and $^{26}Mg/^{24}Mg$ and $^{44}Ca/^{40}Ca$ isotope ratios were measured with ICP-MS (Bruker 820MS) following isotope analysis methods described by van der Heijden et al. (2013a). ICP-MS optimization parameters are summarized in Table 5. The Bruker 820MS instrument is equipped with a collision/reaction cell. In order to eliminate the ^{40}Ar interference to measure ^{40}Ca, a H_2 reaction gas was used: H_2 was injected directly into the plasma (100 mL min^{-1}). The H_2 gas reacts with Ar^+ ions and forms a neutral species which does not enter the mass spectrometer portion of the instrument. All Mg and Ca isotope ratios were analysed separately. Because the response of the detector to sample concentration was not linear, all samples were diluted or evaporated to the same concentration: 100 ppb Mg or 100 ppb Ca. Instrument mass bias was corrected for using the standard bracketing technique. Mg mass bias was corrected by inserting the NIST SRM-980 standard every 12 samples. Because the response of the detector was not linear with the ^{44}Ca enrichment of samples, Ca mass bias was corrected by inserting both the NIST 915b standard and an in-house ^{44}Ca-enriched standard ($\delta^{44}Ca = 1{,}880$ ‰) every 12 samples. The precision, repeatability and accuracy of the ICP-MS methods was determined in van der Heijden et al. (2013a). $^{26}Mg/^{24}Mg$ ratio measurement precision, repeatability and accuracy were respectively 2.0, 2.0 and 0.7 ‰ and 3.2, 3.7 and 1.2 ‰ for $^{44}Ca/^{40}Ca$ ratio measurements. Given natural isotope variations (Cenki-Tok et al. 2009; Farkaš et al. 2011; Holmden and Bélanger 2010; Russell et al. 1978; Wiegand et al. 2005) and ICP-MS measurement precision, a tracer detection limit was set for $\delta^{26}Mg$ and $\delta^{44}Ca$ at 10 ‰ (van der Heijden et al. 2013a).

Table 5 Summary of ICP-MS instrument (Bruker 820MS) optimization parameters for the analysis of $^{26}Mg/^{24}Mg$ and $^{44}Ca/^{40}Ca$

	Magnesium	Calcium
Plasma condition		
RF power (W)	1200	1600
Sampling depth (mm)	5	5
Plasma gas flow (L min^{-1})	15	15
Auxiliary gas flow (L min^{-1})	1.5	1.5
Nebulizer gas flow (L min^{-1})	1	1
Makeup gas flow (L min^{-1})	0.18	0.18
Nebulizer pump (rps)	0.05	0.05
Spray chamber temp (°C)	2	2
Ion lenses		
Extract 1 (V)	−40	−60
Extract 2 (V)	−300	−250
Extract 3 (V)	−400	−400
Corner Lens (V)	−350	−350
Mirror lens left (V)	25	50
Mirror lens right (V)	26	35
Mirror lens bottom (V)	35	35
Entrance plate (V)	−35	−35
Pole bias (V)	−1	−1
Reaction cell		
Sampler H_2 gas flow (mL min^{-1})	0	0
Sampler He gas flow (mL min^{-1})	0	0
Skimmer H_2 gas flow (mL min^{-1})	0	100
Skimmer He gas flow (mL min^{-1})	0	0
Detector		
Points per peak	1	1
Attenuation mode	Medium	No
Acquisistion time/mass (s)	1 (^{24}Mg)	1 (^{40}Ca)
	5 (^{25}Mg)	5 (^{42}Ca)
	5 (^{26}Mg)	5 (^{44}Ca)
Scans/replicate	300	300
Replicates/sample	3	3

Applying the isotopic dilution technique to the whole ecosystem

Principle

The isotopic dilution technique is relatively straight forward. The studied pool is spiked with a given isotope and the concentration of that isotope is measured in that pool. The dilution of the initial isotope spike is then used to measure the size of the

pool and the fluxes that contribute to this pool. The difficulty in ecosystem studies is that ecosystems are composed of many different compartments which are in interaction. The isotopic dilution over the whole ecosystem can only be estimated by averaging measured isotope enrichments in each compartment weighted by the total element pool size of each compartment. The difficulty lies in the fact that the total element pool sizes of each compartment are the unknowns in the equation.

This difficulty was overcome by (i) estimating the total element pool sizes in each compartment (assumption) and then (ii) calculating a "theoretical" isotope enrichment for the whole ecosystem from the mixing of applied tracers with all ecosystem pools [Eq. (7)] and finally (iii) calculating an "experimental" isotope enrichment for the whole ecosystem from measured isotope concentrations in each ecosystem pool [Eq. (8)]. If the "theoretical" and "experimental" isotope enrichment values are different, this may be explained by the fact that the measurements of isotope composition of individual pools may not be representative or that there may be an additional unmeasured pool that has captured some of the tracer. However in this study, if the "theoretical" and "experimental" isotope enrichment values are different, we considered that the initial assumption on total element pool sizes in each compartment was false.

$$\mathrm{Th}\left({}^{Y}X\right) = \frac{\mathrm{Input}\left({}^{Y}X\right)}{B_{\mathrm{est}}(X) + L_{\mathrm{est}}(X) + S_{\mathrm{est}}(X) + \mathrm{Input}(X)} \quad (7)$$

$$\mathrm{Exp}\left({}^{Y}X\right) = \frac{B_{\mathrm{est}}(X) \times B_{\mathrm{est}}\left({}^{Y}X\right) + L_{\mathrm{est}}(X) \times L_{\mathrm{est}}\left({}^{Y}X\right) + S_{\mathrm{est}}(X) \times S_{\mathrm{est}}\left({}^{Y}X\right)}{B_{\mathrm{est}}(X) + L_{\mathrm{est}}(X) + S_{\mathrm{est}}(X)} \quad (8)$$

where ${}^{Y}X$ represents the isotope tracer (i.e. ^{26}Mg or ^{44}Ca), X the total element (i.e. Mg or Ca). Th(${}^{Y}X$) is the "theoretical" and Exp(${}^{Y}X$) the "experimental" isotope enrichment. Input(${}^{Y}X$) is the initially applied tracer amount, $B_{\mathrm{est}}(X)$ is the pool size of element X in tree biomass, $L_{\mathrm{est}}(X)$ is the pool size of element X in the litter-layer, $S_{\mathrm{est}}(X)$ is the pool size of element X in the mineral soil (exchangeable and microbial biomass pools), $B_{\mathrm{est}}({}^{Y}X)$ is the mean ${}^{Y}X$ tracer concentration in tree biomass, $L_{\mathrm{est}}({}^{Y}X)$ the mean ${}^{Y}X$ tracer concentration in the litter-layer and $S_{\mathrm{est}}({}^{Y}X)$ is the mean ${}^{Y}X$ tracer concentration in soil exchangeable and microbial biomass pools. Th(${}^{Y}X$) and Exp(${}^{Y}X$) were then expressed in δ^{26}Mg or δ^{44}Ca (‰).

To determine whether the "theoretical" and "experimental" isotope enrichment values are in agreement, uncertainty, noted $\varepsilon_{\mathrm{exp}}$, in the "experimental" isotopic dilution was estimated by applying Monte-Carlo simulations (n = 1,000). At each iteration, tracer concentrations in the different ecosystem compartments were randomly selected within a normal distribution. The mean and standard deviation of the normal distribution were determined from measured tracer concentration spatial variability. $\varepsilon_{\mathrm{exp}}$ was calculated as the standard deviation of Monte-Carlo simulations (n = 1,000). Agreement or disagreement between "theoretical" and "experimental" isotope enrichment values was as follows:

If the absolute difference, noted Δ_{enrich}, between "theoretical" and "experimental" isotope enrichment values [Eq. (9)] was inferior to $\varepsilon_{\mathrm{exp}}$ both isotope enrichments were considered in agreement and therefore the initial assumption of ecosystem pools was considered valid.

If Δ_{enrich} was superior to $\varepsilon_{\mathrm{exp}}$ both isotope enrichments were considered in disagreement and therefore the initial assumption of ecosystem pools was considered false.

$$\Delta_{\mathrm{enrich}}\left({}^{Y}X\right) = \left|\mathrm{Th}\left({}^{Y}X\right) - \mathrm{Exp}\left({}^{Y}X\right)\right| \quad (9)$$

Calculation methodology

Mg and Ca pools in each compartment in 2012 were estimated from measured pools in 2001 (as described above) and computed fluxes and input–output budgets (Table 3) over the 2003–2008 period (van der Heijden et al. 2013c). However, because these input–output budgets have not been validated with experimental data and given the potential uncertainties around input–output budgets, the input–output budget values

cannot be directly used to estimate Mg and Ca soil pools in 2012.

We applied the isotope dilution theory to determine a range of possible Mg and Ca input–output budget values. To do so, $\Delta_{enrich}(^{Y}X)$ and $\varepsilon_{exp}(^{Y}X)$ were calculated for a range of input–output budgets: from −2.7 to +4 kg ha^{-1} year^{-1} for Mg and from −5 to +5 kg ha^{-1} year^{-1} for Ca. The minimum value of Mg budget range was constrained by the measured exchangeable Mg pool in the soil in 2001 (Table 3) over 12 years the maximum depletion rate is −2.7 kg ha^{-1} year^{-1}. This generated an interval of possible Mg and Ca input–output budgets, noted [Mg_{min}:Mg_{max}] and [Ca_{min}:Ca_{max}]. The input–output budget value for which $\Delta_{enrich}(^{Y}X)$ was minimal [$\Delta_{enrich}(^{Y}X)_{min}$] was considered to be the best estimation of the input–output budget (optimal value of Mg and Ca pools), noted Mg_{opt} and Ca_{opt}.

In order to account for the uncertainty in Mg and Ca pools measured in 2001, a Monte-Carlo approach was applied. The calculation of $\Delta_{enrich}(^{Y}X)$ and $\varepsilon_{exp}(^{Y}X)$ over the range of input–output budgets was repeated 1,000 times and at each iteration, Mg and Ca pools were randomly selected within a normal distribution. From these Monte-Carlo simulations, uncertainty in the estimation of Mg_{min}, Mg_{max}, Ca_{min}, Ca_{max}, Mg_{opt} and Ca_{opt} were calculated from the standard deviations of the 1,000 iterations.

Tracer recovery and uncertainty in tracer pool estimations

Uncertainty in the litter-layer, soil exchangeable and microbial biomass ^{26}Mg and ^{44}Ca pools in March 2012 was estimated from spatial variability [standard deviation of the four soil profiles sampled (Table 4)] of measured isotope enrichment. Uncertainty in the allometric equation predicting ^{26}Mg and ^{44}Ca uptake by trees was assessed using Monte-Carlo simulations (n = 1,000 iterations). At each iteration, tracer uptake for individual trees was randomly selected within the 95 % confidence interval of allometric equations. The tracer uptake of individual trees was summed at the plot scale. Uncertainty in tracer uptake was estimated from the standard deviation of the distribution of the 1,000 iterations.

Tracer recovery was computed from samples collected in March 2012 and was estimated by summing tracer pools of each ecosystem compartment (litter-layer, soil exchangeable, soil microbial biomass and tree biomass). To assess uncertainty in total tracer recovery estimates, a Monte-Carlo procedure was applied. At each iteration, tracer uptake was predicted with the allometric equation (as described above) and a randomly selected value of ^{26}Mg or ^{44}Ca isotope enrichment in the litter-layer, soil exchangeable and microbial biomass was used to computed ^{26}Mg or ^{44}Ca pools in each of these compartments. We assumed that ^{26}Mg and ^{44}Ca isotope enrichments followed a normal distribution (the mean and standard deviation of these distributions were determined from the four soil profile replicates). All ^{26}Mg or ^{44}Ca pools (litter-layer, soil exchangeable, microbial and tree biomass) were then summed and uncertainty was estimated from the standard deviation of the distribution of the 1,000 iterations.

Tracer fluxes in the soil profile

Tracer fluxes in preferential and matrix water flow in the soil profile were calculated by multiplying tracer concentrations in ZTLs (for the preferential flow component) or TCL (for the matrix flow component) by the estimated preferential or matrix water flux at a given depth. The latter was estimated using a lump-parameter hydrological model, BILJOU (Granier et al. 1999), which was calibrated to the beech plot site with a soil moisture data set over 2006–2009 (TDR probes at 15, 30 and 60 cm depth, 5 replicates per depth) and the water tracing experiment with deuterated water (van der Heijden et al. 2013b).

Results

^{26}Mg and ^{44}Ca tracers are presented in this section and "Discussion" section as a percentage of the initially applied tracers. The values of measured isotope ratios in the litter-layer and in the mineral soil are given in Tables 6 and 7.

^{26}Mg and ^{44}Ca tracer recovery in the ecosystem

Tracer recovery in the litter-layer

^{26}Mg and ^{44}Ca tracers were immediately retained in the litter-layer (Fig. 2a). Indeed, one day after the tracing experiment (April 8, 2010), most of the applied tracer

Table 6 Summary of measured isotope ratios (expressed in ‰) in the litter-layer for both exchangeable and total pools

Date	δ^{26}Mg (‰)				δ^{44}Ca (‰)			
	Exchangeable		Total		Exchangeable		Total	
	Mean	STD	Mean	STD	Mean	STD	Mean	STD
08/04/2010	1,226	547	628	159	558	251	468	156
14/04/2010	1,076	377	252	80	611	222	364	39
04/05/2010	870	157	305	63	418	50	292	33
18/05/2010	991	240	302	72	494	219	414	159
15/06/2010	834	72	343	107	492	60	335	23
15/07/2010	983	263	182	102	567	366	450	207
10/08/2010	713	95	126	48	581	211	344	113
08/09/2010	658	45	183	31	428	52	300	22
04/10/2010	759	158	172	74	400	64	403	176
04/11/2010	721	105	199	99	601	208	448	152
03/01/2011	647	78	139	69	547	122	439	91
22/02/2011	756	316	146	29	650	366	543	312
22/03/2011	656	69	278	63	455	108	436	69
19/04/2011	524	125	177	89	390	98	356	111
16/05/2011	555	200	224	158	440	143	404	139
11/07/2011	434	209	115	33	420	191	322	171
05/09/2011	445	116	114	19	312	88	360	118
30/11/2011	351	52	74	14	340	142	256	23
22/03/2012	196	17	60	22	163	38	154	37

was found in the litter-layer: the total ^{26}Mg and ^{44}Ca pools in the litter-layer represented 80 ± 19 and 106 ± 36 % of applied ^{26}Mg and ^{44}Ca. The release dynamics of both tracers differed. The ^{26}Mg pool decreased rapidly after the application of tracers. 1 week after the application of tracers (April 14, 2010), the total ^{26}Mg pool in the litter-layer only represented 33 ± 10 % of applied ^{26}Mg. Thereon, the ^{26}Mg pool in the litter-layer decreased progressively but at a much slower rate. The release of ^{44}Ca from the litter-layer was much slower than ^{26}Mg. The retained ^{44}Ca pool only slightly decreased during the first year (68 ± 26 % of ^{44}Ca was still retained in April 2011) and decreased during the second year. 2 years after the tracing experiment (March 2012), this resulted in a much higher proportion of applied ^{44}Ca still retained in the litter-layer: 8.0 ± 3.0 % of ^{26}Mg and 32.8 ± 8.6 % of ^{44}Ca.

^{26}Mg and ^{44}Ca tracers were mainly retained on the cationic exchange capacity of the litter-layer (Fig. 2b). On average over the study period, litter CEC extractable ^{26}Mg and ^{44}Ca pools represented respectively 90 ± 17 and 82 ± 35 % of total ^{26}Mg and ^{44}Ca pools litter (measured by acid digestion).

Tracer recovery in the mineral soil

Soil microbial immobilization of base cations Throughout the study period (April 2010–March 2012), the comparison of fumigated and unfumigated soil CEC extractions (Fig. 3) evidenced a high immobilization of Mg in soil micro-organisms. Indeed, Mg levels in fumigated samples were on average 2.2-fold higher than in unfumigated samples. Anova tests showed that the differences were statistically significant for all depths down to 30 cm (Table 8). K levels in fumigated samples were also higher (1.4-fold on average) than in unfumigated samples. However, differences were only significant in the 0–15 cm soil layer. No difference was observed between fumigated and unfumigated Ca extractions.

The isotopic composition of fumigated–unfumigated extractions was also compared (Fig. 3). Isotopic composition of unfumigated extractions tended to be

Table 7 Summary of measured isotope ratios (expressed in ‰) in the mineral soil layers for both non-fumigated and fumigated soil CEC extractions

Date	Layer (cm)	δ^{26}Mg (‰)				δ^{44}Ca (‰)			
		Non-fumigated		Fumigated		Non-fumigated		Fumigated	
		Mean	STD	Mean	STD	Mean	STD	Mean	STD
04/05/2010	0–2.5	334	317	191	219	88	96	109	109
	2.5–5	317	414	173	190	100	131	115	135
	5–7.5	191	120	106	74	54	32	52	34
	7.5–10	141	133	63	48	44	57	43	49
	10–15	75	87	29	28	32	36	27	22
04/11/2010	0–2.5	560	257	523	213	277	125	286	133
	2.5–5	299	278	251	188	140	107	133	112
	5–7.5	193	168	152	102	95	74	83	56
	7.5–10	153	84	124	57	70	28	62	20
	10–15	158	82	118	45	100	93	92	84
	15–20	57	37			27	29		
	20–25	26	10			10	2		
	25–30	16	17			8	2		
05/09/2011	0–5	484	189	388	160	296	165	290	147
	5–10	246	103	198	105	135	87	133	84
	10–15	181	106	142	82	91	87	95	80
	15–20	110	88	109	78	46	54	50	46
	20–25	92	70	81	68	18	19	25	18
	25–30	48	38	53	28	10	7	9	7
22/03/2012	0–5	476	55	455	76	342	91	333	97
	5–10	308	106	244	95	194	111	166	100
	10–15	162	4	123	16	62	15	47	10
	15–20	115	43	95	40	28	27	20	14
	20–25	99	41	79	47	15	15	30	49
	25–30	103	58	90	54	18	18	10	13
	30–35	96	49			19	19		
	35–40	78	49			11	26		
	40–45	52	35			0	4		
	45–50	46	22			4	7		
	50–55	27	10			−3	4		
	55–60	23	13			−3	4		

more enriched in ^{26}Mg than fumigated extractions. The difference was statistically significant for the 0–10 cm layer. The ^{26}Mg enrichment of unfumigated samples was on average 1.6-fold higher than fumigated samples for the 0–10 cm layer. No difference was observed between the isotopic composition of fumigated and unfumigated Ca extractions.

Tracer recovery in the mineral soil over time While the amount of ^{26}Mg and ^{44}Ca retained in the litter-layer decreased, the amount of ^{26}Mg and ^{44}Ca retained in the soil (soil exchangeable and microbial biomass pool) increased during the 2 years after the tracing experiment (Figs. 4, 5). In the present study, four dates were selected to best represent the dynamics of

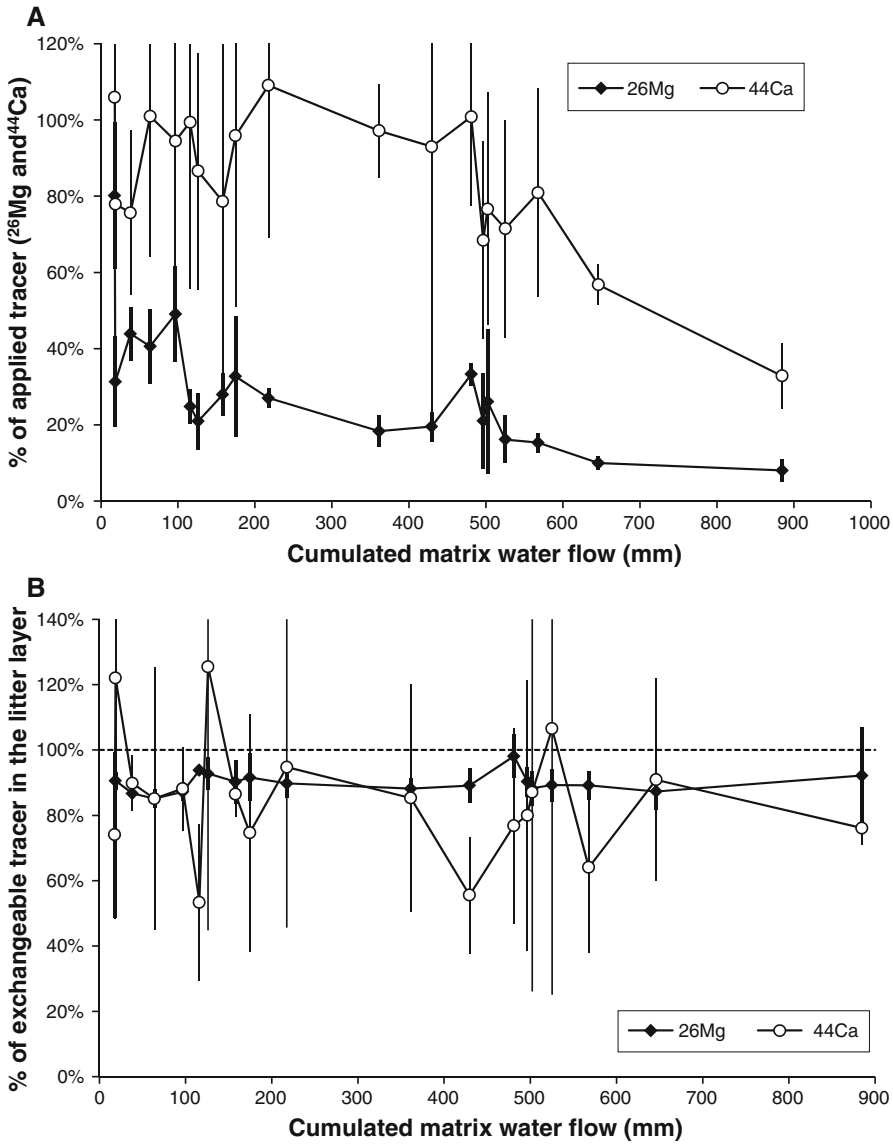

Fig. 2 Excess ^{26}Mg and ^{44}Ca pools in the litter-layer during the 2 years after the tracing experiment. **a** The total ^{26}Mg and ^{44}Ca pools in the litter-layer (measured by HNO_3 digestion) plotted against cumulated matrix water flow since the application of tracers (mm) (van der Heijden et al. 2013b) expressed in percentage of applied tracers. **b** The percentage of exchangeable ^{26}Mg and ^{44}Ca in the litter pool: (exchangeable ^{26}Mg or ^{44}Ca litter pool)/(total ^{26}Mg or ^{44}Ca litter pool). In both figures, *error bars* are standard deviations at each sampling date. Correspondence between sampling dates and cumulated matrix water flow is given in Table 4

retention of ^{26}Mg and ^{44}Ca in the soil profile: May 2010 (beginning of the first vegetation season), November 2010 (after the first vegetation season), September 2011 (after the second vegetation season) and March 2012 (2 years after the application of tracers).

In May 2010, ~33 % of applied ^{26}Mg was retained in the soil profile (Fig. 4). 2 years later (March 2012), 67 % of applied ^{26}Mg was found in the soil profile. Between May 2010 and March 2012, ^{26}Mg in the soil profile increased by ~34 % while ^{26}Mg in the litter-layer decreased by ~33 %. A considerable amount of ^{26}Mg was rapidly retained in the 0–5 cm layer: in May 2010 ~24 % of applied ^{26}Mg. The amount of ^{26}Mg retained in the 0–5 cm layer increased until November 2010 (~37 %) and then remained stable until March 2012. ^{26}Mg transferred slowly downwards in the soil profile during the 2 years and ^{26}Mg pools in the deeper soil layers increased progressively. A small proportion of ^{26}Mg was immobilized in microbial biomass in May 2010 (~4 %). However, this value increased until autumn 2010 (~16 %) and remained stable thereon. Microbial biomass immobilized ^{26}Mg in the 0–30 cm layer however the 0–5 cm layer represented ~50 % of total immobilized ^{26}Mg in soil microbial biomass.

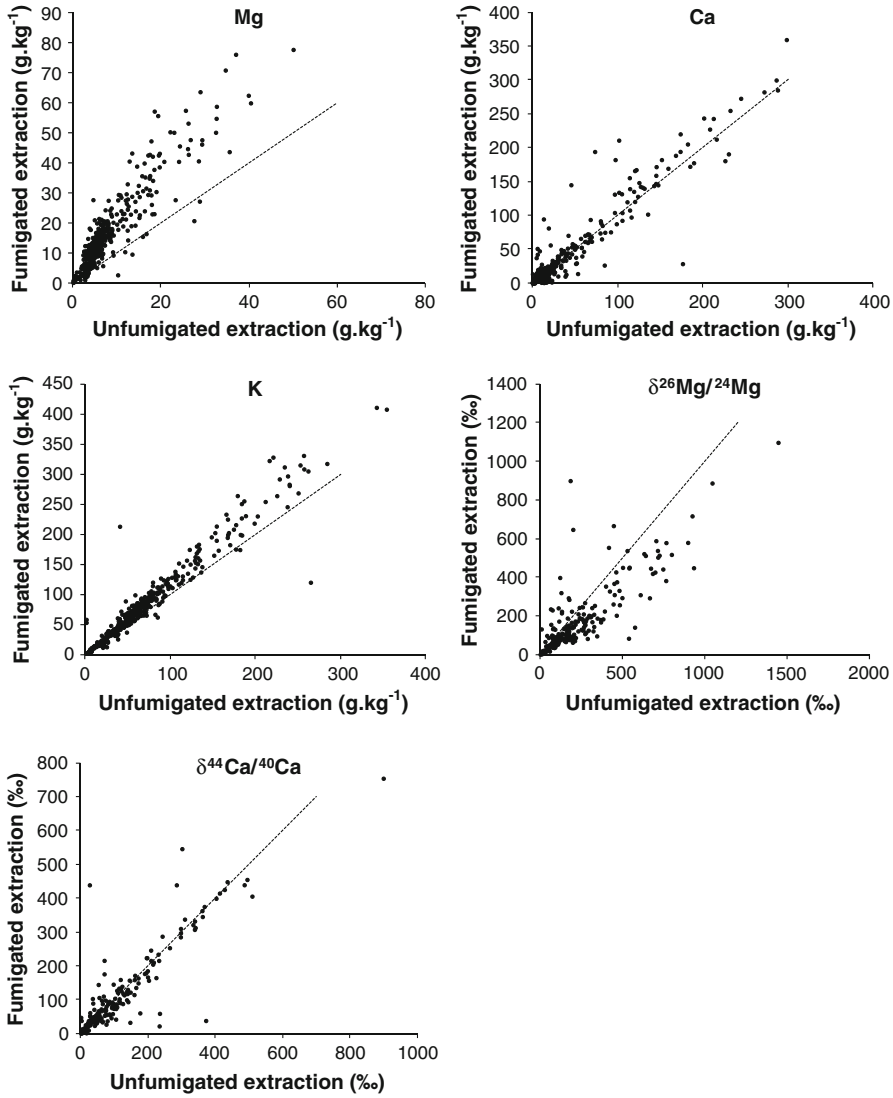

Fig. 3 Differences between fumigated and unfumigated soil extractions for total element (Mg, Ca and K), expressed in g kg^{-1}, and stable isotope tracers (^{26}Mg and ^{44}Ca) expressed in ‰. The *dotted line* is the 1:1 line

Table 8 Differences between fumigated and unfumigated extractions for total element (Mg, Ca and K) and isotopic composition ($^{26}Mg/^{24}Mg$ and $^{44}Ca/^{40}Ca$) tested by ANOVA for soil samples collected from 04/2010 to 04/2012

Depth	Mg	Ca	K	$\delta^{26}Mg/^{24}Mg$	$\delta^{44}Ca/^{40}Ca$
0–5	>0.0001	0.4935	0.0128	0.0188	0.8661
5–10	>0.0001	0.8304	>0.0001	0.0008	0.5255
10–15	>0.0001	0.3308	0.0080	0.1286	0.7773
15–20	0.0015	0.8414	0.3897	0.4179	0.5844
20–25	0.0013	0.5582	0.2181	0.8812	0.1316
25–30	0.0066	0.5851	0.1990	0.8469	0.9452

The *p* value of the ANOVA tests is presented for each element and for each depth from 0 to 30 cm depth

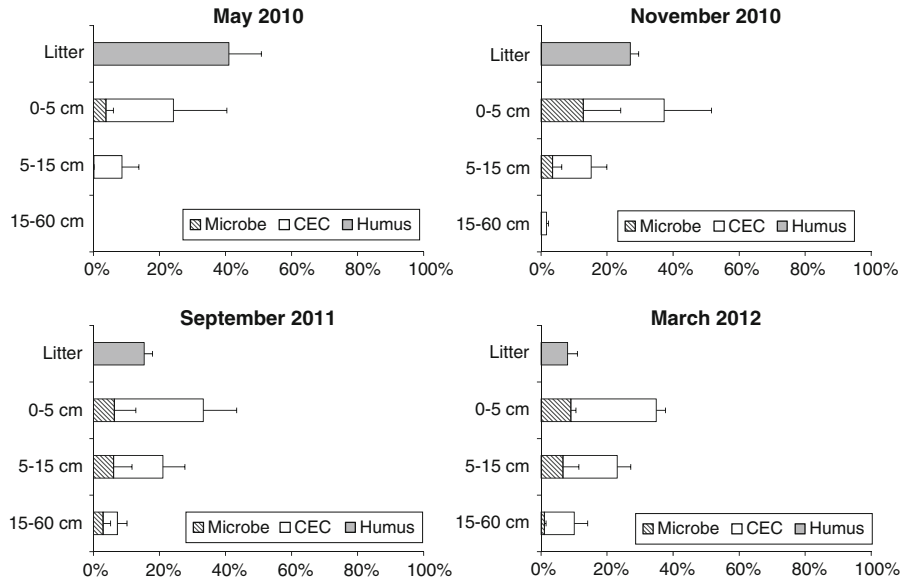

Fig. 4 Excess ^{26}Mg in the litter-layer (total ^{26}Mg in litter measured by HNO_3 digestion), the soil exchangeable and microbial biomass pools in the different soil layers (0–5, 5–15 and 15–60 cm) during the 2 years after the tracing experiment expressed in percentage of applied tracers. *Error bars* represent standard deviations

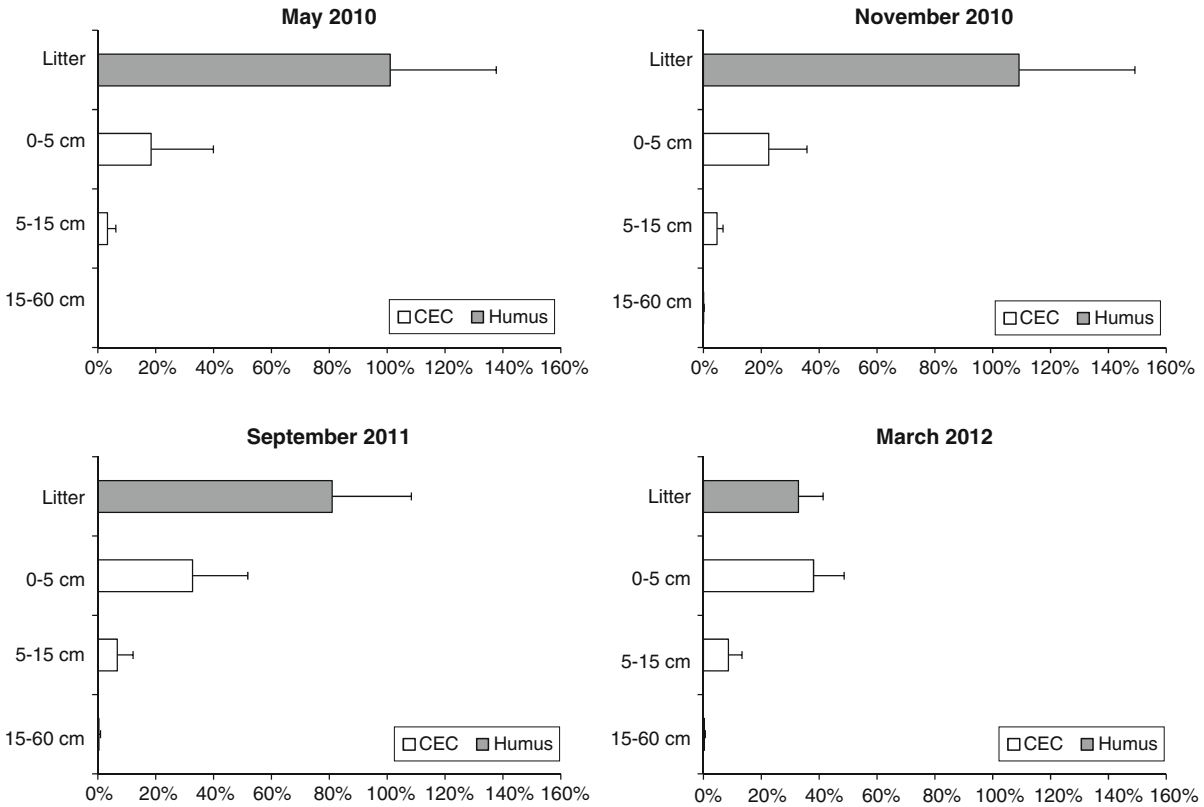

Fig. 5 Excess ^{44}Ca in the litter-layer (total ^{44}Ca in litter measured by HNO_3 digestion), the soil exchangeable and microbial biomass pools in the different soil (0–5, 5–15 and 15–60 cm) during the 2 years after the tracing experiment expressed in percentage of applied tracers. *Error bars* represent standard deviations

The ^{44}Ca pool in the soil profile increased throughout the 2 years from ~22 % in May 2010 to ~47 % in March 2012 (Fig. 5), while the ^{44}Ca pool in the litter-layer decreased by ~68 %. ^{44}Ca was mainly retained in the 0–5 cm layer (38.1 ± 10.5 %) and only small amounts transferred to deeper soil layers.

Tracers in the soil solution

Soil solutions collected with ZTLs at 0 and 10 cm depth Soil solutions collected with ZTL at both 0 cm (below the litter-layer) and 10 cm depth were highly enriched in ^{26}Mg and ^{44}Ca (Fig. 6). δ^{26}Mg and δ^{44}Ca were highest just after the tracing experiment: at 0 cm, δ^{26}Mg ≈ 3,000 ‰ and δ^{44}Ca ≈ 1,400 ‰ and at 10 cm depth, δ^{26}Mg ≈ 2,300 ‰ and δ^{44}Ca ≈ 1,400 ‰. δ^{26}Mg and δ^{44}Ca decreased until January 2011 (361 mm of cumulated matrix water flow) but thereon remained relatively stable only slightly decreasing over time: at 0 cm, δ^{26}Mg ≈ 500 ‰ and δ^{44}Ca ≈ 250 ‰ and at 10 cm depth, δ^{26}Mg ≈ 300 ‰ and δ^{44}Ca ≈ 200 ‰. Spatial and temporal variability was much higher in the ZTL collectors at 0 cm than at 10 cm. At both 0 and 10 cm depth, δ^{2}H was highest just after the tracing experiment and rapidly decreased until August 2010. Thereon δ^{2}H at both 0 and 10 cm depth was close to natural abundance <0 ‰.

Soil solutions collected with TCL at 15 and 30 cm depth The separation of ^{26}Mg and ^{44}Ca elution peaks from the ^{2}H elution peak was expressed with the difference (noted $\Delta_{Mg-water}$ and $\Delta_{Ca-water}$) of cumulated matrix water flow (mm) between the occurrence of the ^{26}Mg or ^{44}Ca elution peak and the ^{2}H elution peak.

At 15 cm depth, each TCL replicate showed a different sequence of ^{26}Mg, ^{44}Ca and ^{2}H elution peaks (Fig. 7). *Replicate 15.1* The ^{26}Mg and ^{44}Ca elution peak were separated from ^{2}H: $\Delta_{Mg-water} = +347$ mm and $\Delta_{Ca-water} = +153$ mm. *Replicate 15.2* The ^{26}Mg elution peak was well separated from the ^{2}H peak

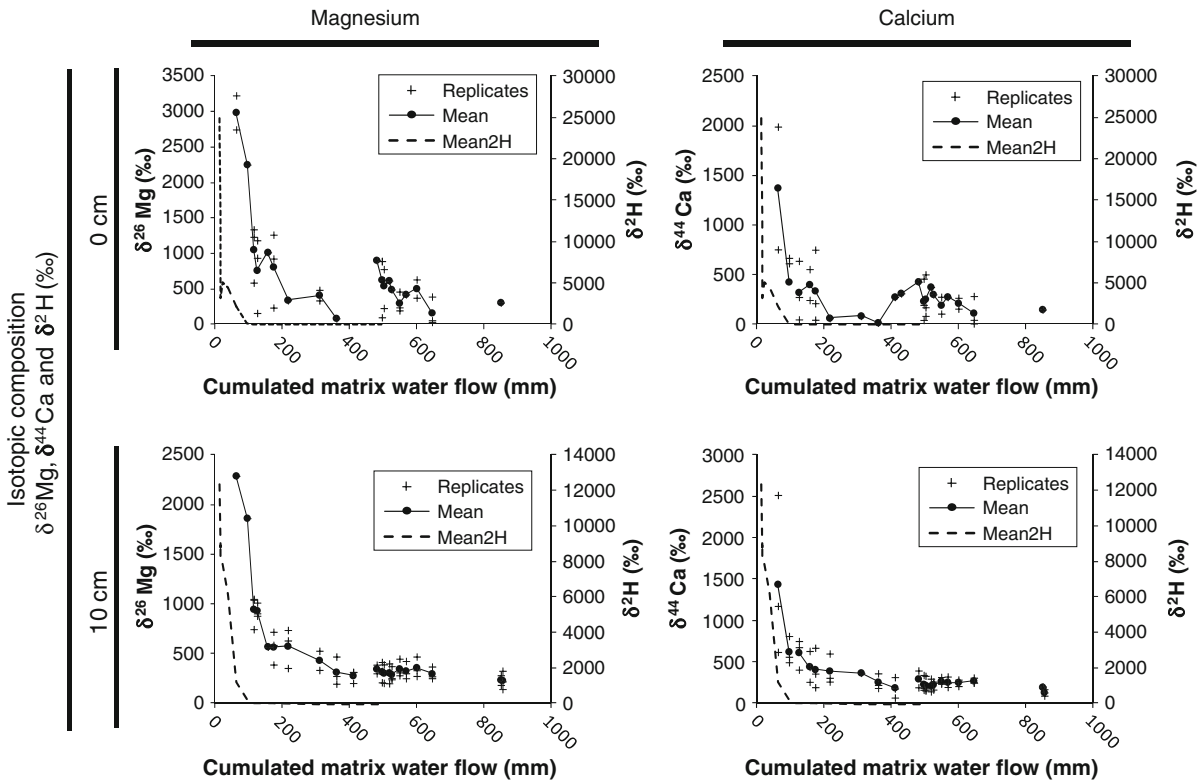

Fig. 6 Isotopic composition (δ^{2}H, δ^{26}Mg and δ^{44}Ca) of soil solution collected with ZTLs at 0 and 10 cm depth plotted against cumulated matrix water flow since the application of tracers (mm) (van der Heijden et al. 2013b). *Crosses* represent individual replicates and *circles* represent the mean value at each sampling date. Correspondence between sampling dates and cumulated matrix water flow is given in Table 4

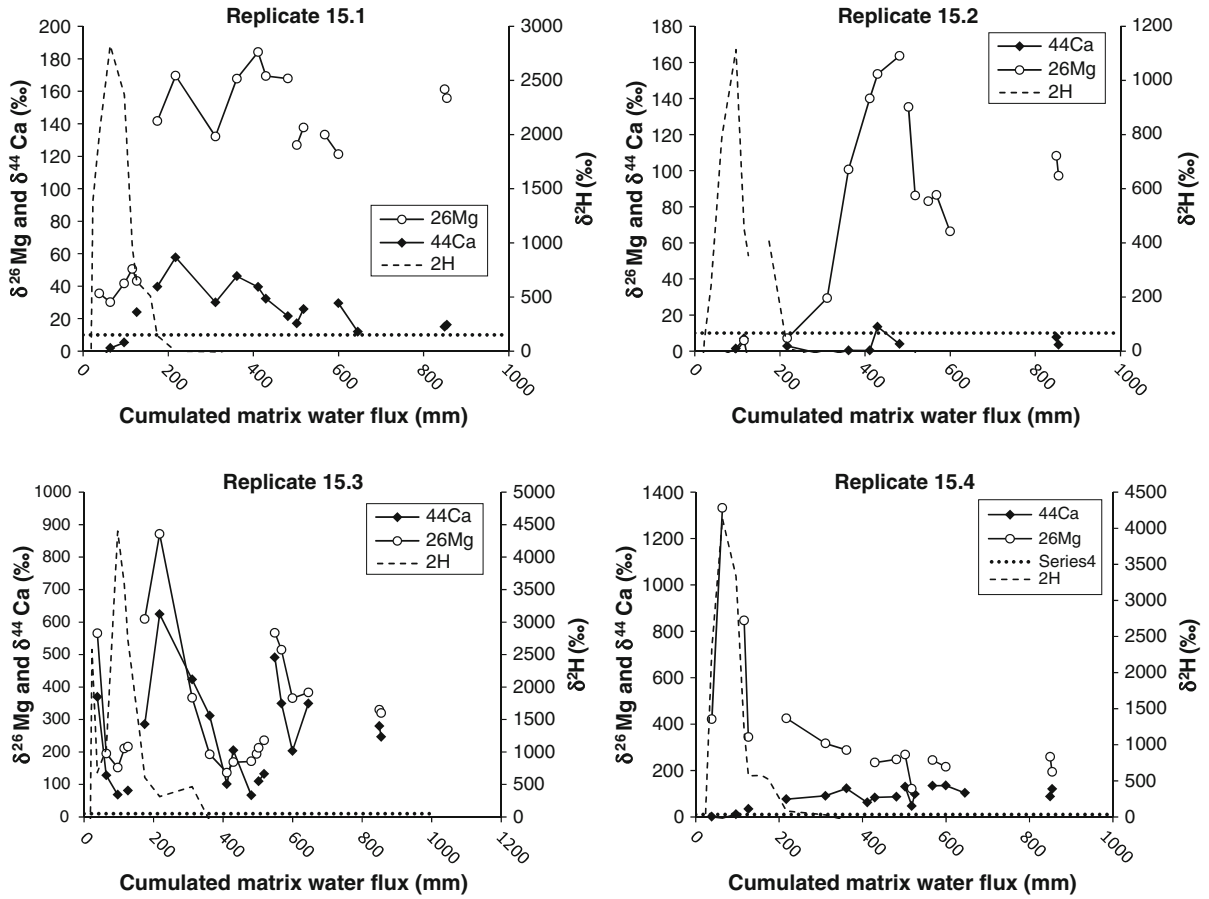

Fig. 7 Isotopic composition (δ^2H, δ^{26}Mg, δ^{44}Ca) of soil solution collected with TCL at 15 cm depth plotted against cumulated matrix water flow since the application of tracers (mm) (van der Heijden et al. 2013b). The *horizontal dotted line* represents the analytical detection limit for excess ^{26}Mg and ^{44}Ca (10 ‰). Correspondence between sampling dates and cumulated matrix water flow is given in Table 4

($\Delta_{Mg-water} = +383$ mm). δ^{44}Ca was below the detection throughout the study period. *Replicate 15.3* High δ^{26}Mg and δ^{44}Ca were observed simultaneously to this first ^{2}H peak. A second ^{2}H elution peak was observed and a second ^{26}Mg and ^{44}Ca elution peak also occurred but was separated from the second ^{2}H peak ($\Delta_{Mg-water} = +120$ mm and $\Delta_{Ca-water} = +120$ mm). *Replicate 15.4* A ^{26}Mg elution peak occurred simultaneously with the ^{2}H peak ($\Delta_{Mg-water} = 0$ mm). The ^{44}Ca elution peak was well separated from ^{2}H: δ^{44}Ca increased progressively during the study period and the maximum of the elution peak could not be distinguished.

At 30 cm depth, spatial variability was less pronounced for both ^{26}Mg and ^{44}Ca. Replicates 30.1, 30.2 and 30.4 showed a similar sequence of ^{26}Mg, ^{44}Ca and ^{2}H elution peaks (Fig. 8). δ^{26}Mg exceeded the detection limit after ~410 mm (January 2011), ~311 mm (December 2010) and ~430 mm (February 2011) in replicates 30.1, 30.2 and 30.4 respectively. δ^{26}Mg increased progressively during the study period for all three replicates. A ^{26}Mg peak occurred after 480 and 600 mm (March–October 2011) in all three replicates. However, this event only represented the maximum of the elution peak for replicate 30.1. δ^{44}Ca remained under the detection limit until October 2011 (~600 mm). Beyond that date, low δ^{44}Ca was observed in replicate 30.2 (~35 ‰). And no data was available for replicate 30.1 and 30.4. *Replicate 30.3* The ^{26}Mg elution peak occurred simultaneously to the ^{2}H peak. δ^{26}Mg was maximum at the beginning

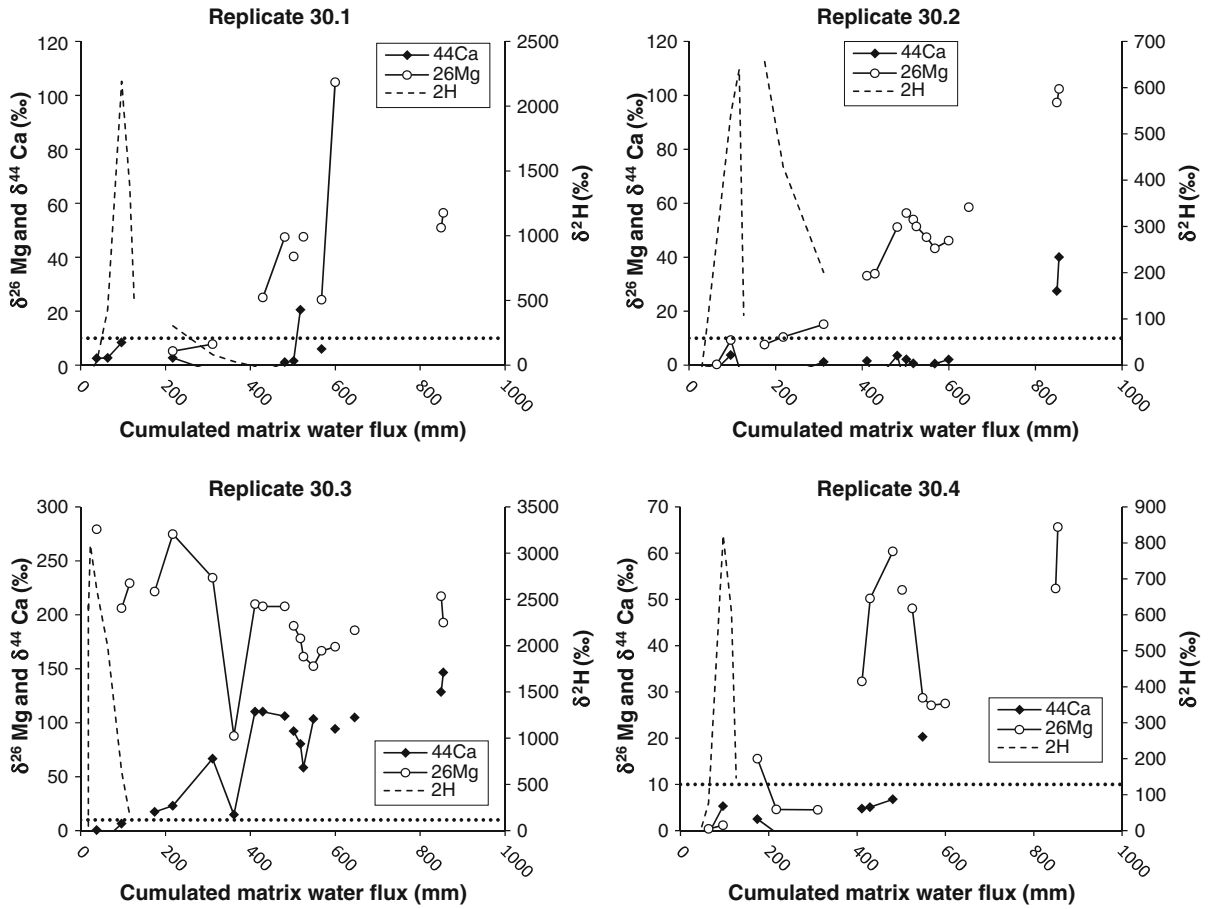

Fig. 8 Isotopic composition (δ^2H, δ^{26}Mg and δ^{44}Ca) of soil solution collected with TCL at 30 cm depth plotted against cumulated matrix water flow since the application of tracers (van der Heijden et al. 2013b). The *horizontal dotted line* represents the analytical detection limit for excess ^{26}Mg and ^{44}Ca (10 ‰). Correspondence between sampling dates and cumulated matrix water flow is given in Table 4

of the study period and decreased continuously thereafter. δ^{44}Ca exceeded the detection limit in October 2010 ($\sim$175 mm) and increased progressively throughout the study period. δ^{26}Mg and δ^{44}Ca in replicate 30.3 were much higher than the other replicates. At 60 cm depth and throughout the monitoring period, δ^{26}Mg and δ^{44}Ca in all replicates were below the detection limit (data not shown).

^{2}H, ^{26}Mg and ^{44}Ca tracer flow velocities (millimeter of tracer displacement per millimeter of percolated water) were computed using the cumulated matrix water flow at the maximum of the elution peak (Table 9). Because no elution peak could be identified (either δ^{44}Ca values were below detection limit or the highest δ^{44}Ca values were at the end of the study period) for many replicates at both 15 and 30 cm depth, maximum velocities were computed.

Tracer recovery in tree biomass

Total immobilized ^{26}Mg and ^{44}Ca in each sampled tree was measured and plotted against tree circumference at breast height (Fig. 9). For both ^{26}Mg and ^{44}Ca, the relation between tracer immobilization and tree circumference was linear. For one sampled tree, both ^{26}Mg and ^{44}Ca immobilization was particularly low and did not follow the main linear relation. This sampled tree was considered as an outlier when fitting linear models to predict tracer uptake (Table 10).

Table 9 ^{2}H, ^{26}Mg and ^{44}Ca transfer velocity in the soil profile (mm of tracer displacement per mm of cumulated matrix water flow) (van der Heijden et al. 2013b)

	Flow velocity (mm mm^{-1})			
	Rep 1	Rep 2	Rep 3	Rep 4
15 cm				
^{2}H	2.3	1.6	1.6	2.3
^{26}Mg	0.4	0.3	0.7	2.3
^{44}Ca	0.7	<0.2	0.7	<0.2
30 cm				
^{2}H	3.2	1.7	13.6	3.2
^{26}Mg	0.5	0.4	1.4	0.4
^{44}Ca	<0.4	<0.4	<0.4	<0.4

Transfer velocities were computed using the maximum of elution peaks in soil solutions collected at 15 and 30 cm with tension-cup lysimeters

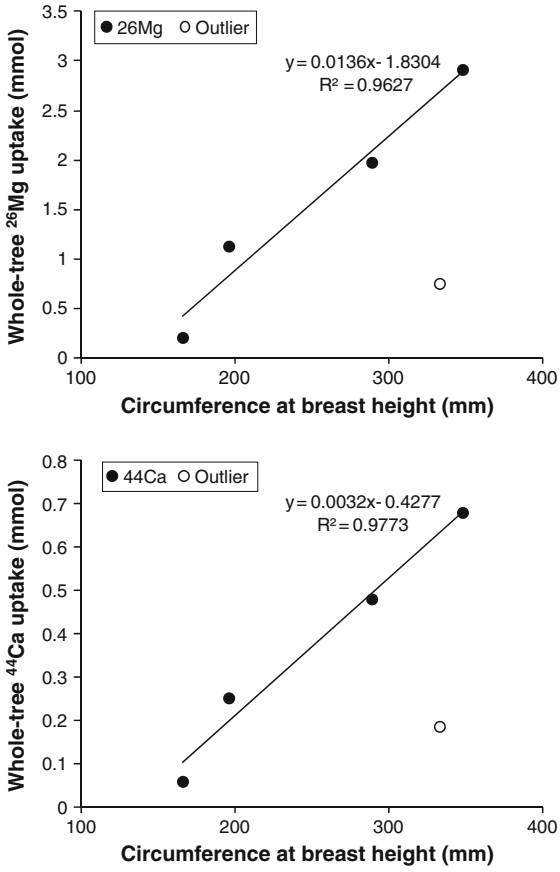

Fig. 9 Relation between whole-tree ^{26}Mg and ^{44}Ca uptake (expressed in mmol of tracer) during the 2 years following the application of the tracer and tree circumference at breast height (mm). One sampled tree presented abnormally low tracer uptake and was considered as an outlier to fit allometric equations

^{26}Mg and ^{44}Ca immobilization in the whole-tree (above and below-ground organs) was positively correlated to tree circumference.

Tracer recovery in the whole ecosystem

To compute tracer recovery, Mg and Ca input–output budgets over 2001 and 2012 were assumed to be −0.8 and 0 kg ha^{-1} year^{-1} respectively. These budgets were applied to measured soil pools in 2001 to compute Mg and Ca pools in 2012. In March 2012 (Fig. 10), 27 ± 9 and 21 ± 6 % of the applied ^{26}Mg and ^{44}Ca were immobilized in tree biomass (above-ground and root biomass). Most of the accounted ^{26}Mg and ^{44}Ca tracer recovery was found in the soil profile (litter-layer, exchangeable and microbial biomass pools) 74 and 80 %. The litter-layer still contained 8.0 ± 3 and 33 ± 9 % and the microbial biomass immobilized a high amount of ^{26}Mg (17 ± 6 %) while immobilized ^{44}Ca in microbial biomass was nil. Finally, the soil exchangeable pool (0–60 cm) contained 50 ± 3 and 47 ± 14 % of applied ^{26}Mg and ^{44}Ca. The investigation of the different ecosystem compartments (litter-layer, exchangeable, microbial and tree biomass) accounted for 102 ± 3 and 100 ± 18 % of the applied ^{26}Mg and ^{44}Ca.

Mg and Ca pool size change tested with the isotopic dilution technique

Applying the isotope dilution theory enabled to estimate Mg and Ca input–output budgets over the 2001–2012 period (Fig. 11). "Theoretical" and "experimental" isotope enrichment values for the whole ecosystem were in agreement [i.e. $\Delta_{enrich}(^{26}Mg)$ and $\Delta_{enrich}(^{44}Ca)$ inferior to $\varepsilon(^{26}Mg)$ and $\varepsilon(^{44}Ca)$] for Mg budgets between −1.2 ± 0.1 and −0.6 ± 0.1 kg ha^{-1} year^{-1} and for Ca budgets between −2 ± 1.2 and + 3.2 ± 1.2 kg ha^{-1} year^{-1}. Δ_{enrich} (^{26}Mg) was minimal for a Mg budget equal to −0.9 ± 0.1 kg ha^{-1} year^{-1}. $\Delta_{enrich}(^{44}Ca)$ was minimal for a Ca budget equal to 0 ± 1.2 kg ha^{-1} year^{-1}.

Mg and Ca input–output budgets calculated from conventional methods (van der Heijden et al. 2013c) were reported in Fig. 11. The conventional Mg I/O budget was within the [Mg_{inf}:Mg_{sup}] interval but also within the uncertainty interval around Mg(Δ_{min}). The conventional Ca I/O budget was however outside the

Table 10 Linear regression model parameters for the allometric equations predicting whole-tree ^{26}Mg and ^{44}Ca uptake (mmol) from breast height tree circumference (BHC) (mm)

Tracer	Parameters	Value	SD	Pr > t	R^2
^{26}Mg	Intercept	−1.83E+00	4.91E−01	0.065	
	BHC	1.36E−02	1.89E−03	0.019	0.963
^{44}Ca	Intercept	−4.28E−01	8.94E−02	0.041	
	BHC	3.19E−03	3.44E−04	0.011	0.977

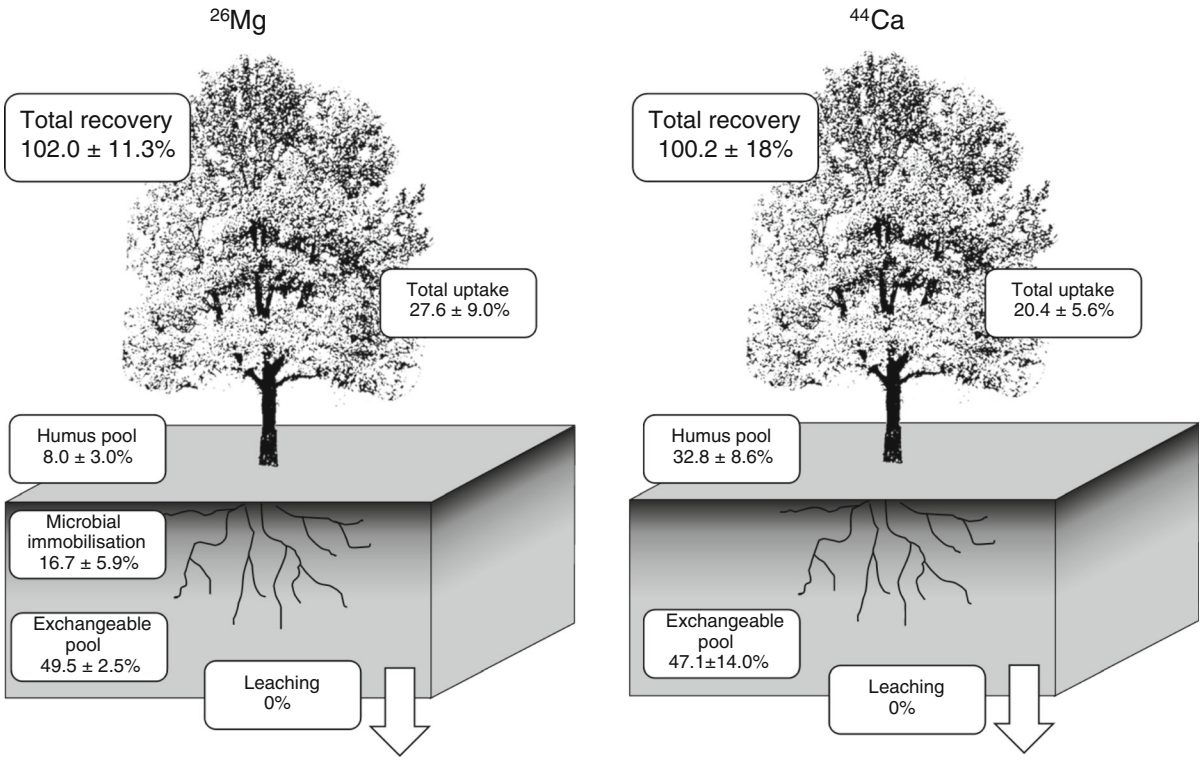

Fig. 10 ^{26}Mg and ^{44}Ca tracer total recovery and tracer distribution in ecosystem compartments 2 years after the application of tracers. ^{26}Mg and ^{44}Ca tracers are expressed in percentage of the applied tracer (mean ± standard deviation)

[Ca_{inf}:Ca_{sup}] interval but within the uncertainty interval around Ca_{inf}.

Discussion

Soil exchangeable Mg and Ca pool change over time

Although the isotopic dilution technique is a well-known technique and has been applied to quantify many different elements in many different systems (Achat et al. 2009a, b; Cookson and Murphy 2004; Forbes and Perley 1951; Stroud et al. 2011; von Hevesy and Hofer 1934; Willison et al. 1998), we present here, to our knowledge, the first isotopic dilution technique applied to the whole ecosystem to assess Mg and Ca pool size change. This enabled to determine the range of soil exchangeable Mg and Ca pool size change between 2001 and 2012 (Fig. 11).

The results show that Mg was depleted from the soil exchangeable pool between 2001 and 2012 and suggest that the Mg depletion rate was between −1.2 and −0.6 kg ha^{-1} $year^{-1}$ but was most likely

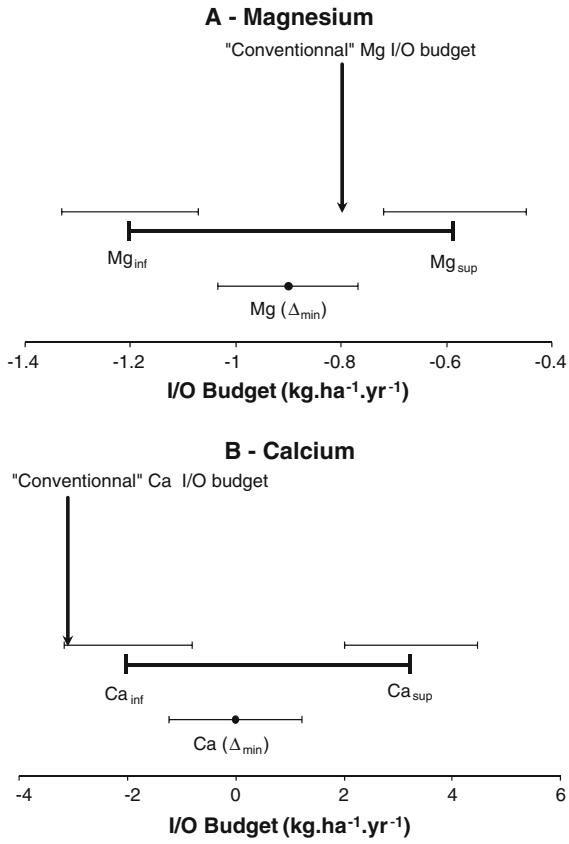

Fig. 11 Range of possible values for Mg and Ca input–output budgets according to the isotopic dilution theory. The *vertical arrows* indicate computed input–output budgets over 2003–2008 (van der Heijden et al. 2013c)

-0.9 ± 0.1 kg ha^{-1} year^{-1} [Mg(Δ_{min})]. This value was very similar to Mg depletion estimated from conventional input–output Mg budgets, -0.8 kg ha^{-1} year^{-1} (van der Heijden et al. 2013c). It is thus likely that computed input–output Mg budgets are valid.

The isotopic dilution results for Ca were less evident. Results suggested that Ca input–output budgets may have ranged from -2 to $+3.2$ kg ha^{-1} year^{-1}. However, results also suggest that the Ca budgets were most likely close to 0 ± 1.2 kg ha^{-1} year^{-1}. The results from the isotopic dilution therefore seem in disagreement with conventional input–output Ca budgets (i.e. -3.1 kg ha^{-1} year^{-1}). Although within uncertainty in the estimation of Ca_{inf}, we cannot assert that conventional Ca budgets are not valid. However, our results strongly suggest that conventional Ca budgets were in fact false and that Ca depletion did not occur over the 2001–2012 period. Indeed, the conventional Ca budget value was very close to lower limit of the confidence interval around Ca_{inf} and very different from Ca(Δ_{min}). We therefore hypothesize that no Ca depletion occurred over the 2001–2012 period. This implies that either Ca inputs to the soil are underestimated, or Ca outputs are over-estimated, or a combination of these factors.

It seems more likely that Ca inputs were underestimated. Indeed, an over-estimation of the leaching flux (1.4 kg ha^{-1} year^{-1}) cannot by itself equilibrate Ca budgets. Furthermore, it seems unlikely that the leaching or uptake flux were well measured for one element but not for the other. It is possible that a Ca weathering source was not taken into account. Indeed, weathering rates were estimated using the PROFILE model and the soil mineralogy but the latter doesn't take into account amorphous minerals which may represent an important source of nutrients (Yanai et al. 2005). Another possible Ca-input to the ecosystem could be foliar absorption. This process has been evidenced for different plant species (Bukovac and Wittwer 1957; Chishaki et al. 2007; Wittwer and Teubner 1959) however remains difficult to quantify. The midterm monitoring of the tracing plot may enable to investigate and determine which Ca source or sink is responsible for Ca budgets at equilibrium.

Mg depletion may have occurred in the litter-layer and/or in the soil exchangeable pool. A decrease of the soil exchangeable Mg pool is plausible because the isotopic dilution calculations as presented in Fig. 11 was calculated assuming such a decrease. A decrease of Mg and Ca pools in the litter-layer is however unlikely. Indeed, recovery of ^{26}Mg and ^{44}Ca in the litter-layer the day following the application of tracers (calculated using the Mg and Ca pools in the litter-layer measured in 2001) was close to 100 %: respectively 80 ± 19 and 106 ± 36 %. The spatial variability of ^{26}Mg and ^{44}Ca recovery is mainly due to high spatial variability of nutrient pools in the litter-layer (Bens et al. 2006; Legout et al. 2008). We may therefore assume that the Mg and Ca pools in the litter-layer measured in 2001 are validated.

Overall, our results and methodology show that the isotopic dilution theory may be used to assess nutrient pool size change over time. However, the precision of the results strongly depends on the precision of measurements of total element pool and fluxes in the ecosystem. The spatial variability of nutrient pools in

forest soils is very high limits the extent to which clear conclusion may be drawn from the isotopic dilution theory. Indeed, compared to tracer concentration spatial variability and isotope ratio analyse uncertainty, Mg and Ca pool spatial variability was the major component of isotope dilution uncertainty.

Nevertheless, the dilution of isotopic tracers over time enabled to discuss the validity of computed input–output budgets which would most probably not been possible by resampling the soil in 2012 and performing conventional CEC extractions. Indeed, the spatial variability of soil exchangeable pools measured in 2001 (± 8 kg ha^{-1} Mg and ± 28 kg ha^{-1} Ca) was close to predicted Mg and Ca depletion over 2001–2012 (-8 kg ha^{-1} year^{-1} Mg and -31 kg ha^{-1} year^{-1} Ca). The Monte-Carlo simulations are a complex procedure to set up but were essential in this study to be able to assess that differences between experimental and theoretical isotope enrichments were significantly different and not simply due to uncertainty (isotope ratio spatial variability, total Mg and Ca pools). The isotope dilution calculation methodology presented here may be applied using only average element and isotope pools but such a simplified version would not enable to judge nutrient budgets values.

Fate of Mg and Ca tracers in the forest ecosystem

Retention and release of ^{26}Mg and ^{44}Ca from the litter-layer

High retention of ^{26}Mg and ^{44}Ca in the OL-layer of the litter-layer Organic matter through its' cationic exchange capacity plays an important role in the retention of base cations (Helling et al. 1964; Johnson 2002; Ross et al. 1991; Thompson et al. 1989; Turpault et al. 1996). The cationic exchange capacity of organic matter in the litter-layer is commonly associated with fine fractions of organic matter (OF and OH layers in the litter-layer or soil organic matter) and with the presence of carboxyl groups. In the beech plot, the litter-layer is mainly composed of an OL-layer; OF-layer is very thin and discontinuous, due to heavy swathing before the plantation in 1975. The results from the in situ multi-isotopic tracing experiment show that coarse organic matter (OL layer) rapidly retains Mg and Ca inputs to the soil via rainfall or throughfall (Fig. 2a). The mechanism of retention was mainly ion exchange. Indeed through the study period exchangeable ^{26}Mg and ^{44}Ca pools in the litter pool represented respectively on average 90 ± 17 and 82 ± 35 % of the total ^{26}Mg and ^{44}Ca pools (Fig. 2b). Another possible from of retention could be precipitation of Mg and Ca oxalate crystals (Palviainen et al. 2004; Verrecchia et al. 2006). We may suppose that the coarse OL layer of the litter-layer in our plot has an important cationic exchange capacity. The recovery of the litter CEC extraction protocol used was not measured and was probably below 100 %. Extracting Mg and Ca from the litter CEC may require a different extractant with a higher affinity for organic CEC such as Cu^{2+}. However, ^{26}Mg/^{24}Mg and ^{44}Ca/^{40}Ca isotope ratios in such highly concentrated salt solutions (0.1 mol L^{-1} $CuCl_2$ or 1 mol L^{-1} KCl) could not be analysed on ICP-MS.

Slow release of ^{26}Mg and ^{44}Ca from the litter-layer The pool of immobilized tracers in the litter-layer decreased during the 2 years after the tracing experiment: in March 2012 8 ± 3 % of ^{26}Mg and 33 ± 9 % of ^{44}Ca were still retained in the litter-layer (Fig. 2). As tracers were mainly retained on the cationic exchange capacity of the litter-layer, ^{26}Mg and ^{44}Ca tracers may have been released by two different mechanisms: (1) organic matter mineralization or (2) ion exchange with throughfall.

1 week after the tracing experiment, most of ^{26}Mg initially retained in the litter-layer was released (Fig. 2) while almost 100 % of applied ^{44}Ca was retained in the litter-layer during the first year after the tracing experiment. The different release dynamics may be explained by a much higher affinity of Ca for organic CEC than Mg. This has been reported by many studies (André and Pijarowski 1977; Baes and Bloom 1988; Curtin et al. 1998; DeSutter et al. 2006; Ponette et al. 1997; Salmon 1964). Whereas Ca ions form strong complexes with some organic functional groups, Mg ions mainly bind through electrostatic bonds (Sentenac and Grignon 1981). However, it is likely that a large proportion of Mg was not retained on the organic CEC of the litter-layer but remained in soluble form. Indeed, only 80 ± 19 % of applied ^{26}Mg was retained in the litter-layer after the 16 mm simulated rainfall event (deionised water) and only 31 ± 12 % remained 1 week after the tracing

experiment (18.7 of cumulated rainfall since the application of tracers).

Vertical transfer of Mg and Ca from the topsoil to deeper soil horizons

The soil is a chromatographic column The results from the tracing experiment are evidence that the elution of base cations in soils follows a chromatographic model. Mg was more mobile in the soil profile than Ca and transferred to deeper soil horizons. This was evidenced by the monitoring of the isotopic composition of soil CEC and soil solutions. Significant ^{26}Mg amounts were observed below 15 cm depth as soon as November 2011 (Fig. 4), whereas very little ^{44}Ca ($\sim$1 %) was found below 15 cm after 2 years (Fig. 5). This was reflected by the mapping of tracers in the soil profile in March 2012: $\sim$33 % of ^{26}Mg and only $\sim$9 % of ^{44}Ca was found below 5 cm depth, $\sim$15 % of ^{26}Mg was found below 15 cm depth. The difference of vertical transfer velocities (Table 9) of Mg and Ca was also evidenced by the monitoring of the isotopic composition of soil solutions at 15 cm and 30 cm depth (Figs. 7, 8). At 15 and 30 cm depth, $\delta^{26}Mg$ was systematically higher than $\delta^{44}Ca$ and ^{26}Mg elution peaks occurred before ^{44}Ca in many cases. Some TCL replicates showed no or very small $\delta^{44}Ca$ throughout the study period.

Johnson (1995) and Johnson et al. (2000) observed a similar chromatographic effect during a Mg and Ca leaching event induced by a pulse of NO_3 both cations peaked simultaneously in the surface soil horizons but separated with depth. Many studies have used chromatographic models to simulate Mg and Ca reactive transport in soil columns (Mansell et al. 1988, 1993). In such models, the separation of Mg and Ca elution peaks is governed by the selectivity coefficients of the cationic exchange capacity ($K_{Ca–Mg}$). $K_{Ca–Mg}$ was not measured for the soil profile of the tracing plot. However, $K_{Ca–Mg}$ have been measured in many different soil types (Table 11) and generally range between 1 and 1.5 indicating a higher affinity of the cationic exchange capacity for Ca.

Sposito and Fletcher (1985), observed $K_{Ca–Mg}$ above 1 for a montmorillonitic soil. Authors argued that Ca–Mg selectivity coefficients of the mineral component of the cationic exchange capacity was likely to be close to 1 (Sposito et al. 1983) and that observed $K_{Ca–Mg}$ in soil samples was probably due to the organic component of the cationic exchange capacity (Fletcher et al. 1984). Indeed, affinity of the organic cationic exchange capacity for Ca is much higher than for Mg (André and Pijarowski 1977; Baes and Bloom 1988; Curtin et al. 1998; DeSutter et al. 2006; Ponette et al. 1997). For instance, Salmon (1964) measured $K_{Ca–Mg} = 5$ in a peat soil (Table 11). Given that most selectivity coefficients presented in Table 11 were measured for agricultural soils with low carbon content, that carbon content is higher in forest soils and at the tracing plot soil in particular (Table 1), it is likely that Ca–Mg selectivity coefficients of the soil in the tracing plot were much higher.

Table 11 Calcium–magnesium selectivity coefficients in different soils

	Selectivity coefficient (Ca–Mg)
Robbins et al. (1980)	
Penoyer loam	1.45
Hunting silty clay loam	1.72
Clark (1970)	
Wyoming bentonite	0.94
Krishnamoorthy and Overstreet (1950)	
Utah bentonite	1.08
Yolo clay	1.42
Paul et al. (1966)	
Oakley soil	1.56
Hanford soil	1.85
Arbuckle soil	1.69
Yolo soil	1.49
Sacremento soil	1.51
Salmon (1964)	
Wyoming bentonite	1.22
Ellsworth illite	1.22
Peat	5.0
Udo (1978)	
Kaolinitic clay	1.47–1.56
Suarez and Zahow (1989)	
Montmorillonite soil	1.12
Sposito and Fletcher (1985)	
Montmorillonite soil	1.18
Gaston et al. (1993)	
Smectitic soils	$\sim$1.0
Momii et al. (1997)	
Farmland loamy sand (aeric haplaquent)	1.55

Indeed, the soil CEC seems to be mainly composed of organic CEC (Table 1). Our results were in agreement with reported proportions of organic CEC in forest ecosystems: 49 % (Thompson et al. 1989), 75–85 % (Oorts et al. 2003), 85 % (Turpault et al. 1996). We hypothesize that soil organic matter and its cationic exchange capacity governed the different Mg and Ca dynamics observed in the soil profile during the multi-isotopic tracing experiment.

It is possible that differences observed between the Mg and Ca in the soil profile may be due to an experimental artifact. Indeed, the average Mg:Ca ratio in throughfall was 0.335 and this ratio was 1.75 in the applied tracing solution. Such a change in the Mg:Ca ratio could modify the behavior of Mg and Ca in the soil. However, in this study, the increased Mg:Ca ratio would favor a higher retention of Mg on the soil CEC. It is therefore probable that the difference in Mg:Ca ratio was buffered by the soil Mg and Ca pools because applied Mg and Ca tracer flux (0.96 and 0.53 kg ha^{-1}) was small compared to soil pools (70 and 264 kg ha^{-1}). When designing multi-isotopic tracing experiments, such parameters (cation ratios and total input flux) need to be considered in order to not disturb the natural processes in cation cycling.

Evidence of rapid and slow transfer of Mg and Ca tracers

The monitoring of soil solutions evidenced different types of Mg and Ca transport in the soil (Figs. 7, 8). The different types of transport observed may be explained by the type of water flow (preferential and matrix flow) and the relative contribution of mineral and soil organic matter to soil CEC. The spatial variability of the different transport types was very high (Fig. 7) and may be explained by the very high spatial variability of soil physical (soil total porosity, pore size distribution…) and chemical properties (soil organic matter content, mineral distribution…). We summarize hereafter the different types of Mg and Ca transport observed:

(1) Rapid transfer with preferential water flow

(i) *Mineral Pipe flow* ^{26}Mg and ^{44}Ca are rapidly transferred through the soil with preferential water flow but interact with the soil CEC which is mainly composed of mineral CEC. The transport of Mg and Ca may thus be delayed compared to the water flux but Mg and Ca elution peaks are not separated ($K_{Ca–Mg} \approx 1$). This type of flow was illustrated by TCL Replicate 15.3.

$$H_2O \geq Mg \approx Ca$$

(ii) *Organic pipe flow* ^{26}Mg and ^{44}Ca are rapidly transferred through the soil with preferential water flow but interact with the soil CEC which is mainly composed of organic CEC. Mg and Ca elution peaks are delayed compared to water due to interaction with the organic CEC which causes the separation of Mg and Ca elution peaks ($K_{Ca–Mg} \gg 1$). This type of flow was illustrated by TCL Replicate 15.4 and 30.3.

$$H_2O \geq Mg > Ca$$

(2) Slow transfer in matrix water flow

(i) *Mineral matrix flow* ^{26}Mg and ^{44}Ca are slowly transferred through the soil with matrix water flow and interact with the soil CEC which is mainly composed of mineral CEC. Mg and Ca are thus delayed compared to the water flux but Mg and Ca elution peaks are not separated ($K_{Ca–Mg} \approx 1$).

$$H_2O \gg Mg \approx Ca$$

(ii) *Organic matrix flow* ^{26}Mg and ^{44}Ca are slowly transferred through the soil with matrix water flow and interact with the soil CEC which is mainly composed of organic CEC. Mg and Ca are thus delayed compared to the water flux and the Ca elution peak is delayed compared to Mg ($K_{Ca–Mg} \gg 1$).

$$H_2O \gg Mg \gg Ca$$

Influence on the nutrient leaching flux

The deuterium water tracing experiment showed that preferential water flow had a strong influence on the deuterium drainage flux (van der Heijden et al. 2013b). In this previous study, the chemical composition of

preferential water flow was estimated from soil solution collected with ZTL at 10 cm depth. Preferential water flow may strongly increase nutrient leaching from the soil profile. However, there was previously no evidence to support the assumption that the chemical composition of preferential water flow does not change with depth.

Throughout the study period, no enrichment above the detection limit was observed in TCL at 60 cm depth (data not shown). The matrix flow component of the ^{26}Mg and ^{44}Ca leaching flux was thus nil. The computed preferential flow component (cumulated tracer flux at 10 cm depth over the 2 years after the application of tracers) of the tracer leaching flux represented 10.7 % of applied ^{26}Mg and 7.7 % of ^{44}Ca. However, there is evidence that the isotopic composition of preferential water flow changed with depth.

(1) No relation was found between δ^{26}Mg and δ^{44}Ca ZTLs at 0 and 10 cm depth.
(2) Isotope enrichments were lower at 10 cm depth than at 0 cm for both Mg and Ca (Fig. 6).
(3) The cumulated ^{26}Mg and ^{44}Ca preferential flux was lower at 10 cm (11 % of applied ^{26}Mg and 8 % of applied ^{44}Ca) than at 0 cm (22 and 14 % respectively).
(4) For TCL in which preferential water flow was evidenced by the deuterium water tracer, ^{26}Mg and ^{44}Ca elution peaks did not always occur simultaneously. For instance, in replicate 15.4 and in replicate 30.3, a ^{26}Mg elution peak associated to preferential water flow occurred but no such peak occurred for ^{44}Ca.
(5) Tracer recovery 2 years after the tracing experiment (102 ± 11 % for ^{26}Mg and 100 ± 18 % for ^{44}Ca) suggests that no leaching of tracers occurred.

Although preferential flow is an important hydrological process that may strongly influence nutrient dynamics and distribution in the soil profile, our results do not support the hypothesis that Mg and Ca are leached with preferential water flow (van der Heijden et al. 2013b). The chemical composition change of preferential water flow with depth may be explained by root uptake along preferential flow paths (Bramley et al. 2003; Martinez-Meza and Whitford 1996) and/or reactive transport of cations along preferential flow paths. However, the separation of ^{26}Mg and ^{44}Ca elution peaks along preferential water flow paths suggests that the main process is reactive transport of cations. Whatever the type of transfer (slow or rapid), Mg and Ca were retained by the soil solid phase.

Tracer uptake The incorporation of ^{26}Mg and ^{44}Ca tracers to the biological cycles of Mg and Ca was surprisingly slow. After 2 years, only 27 ± 9 and 20 ± 6 % of ^{26}Mg and ^{44}Ca respectively were immobilized in tree biomass. Given low Mg and Ca availability in the soil, Mg and Ca tracer inputs were expected to be directly and rapidly immobilized in tree biomass. This being to our knowledge the first in situ ecosystem scale ^{26}Mg and ^{44}Ca tracing experiment, there is no data to compare these results. However ^{26}Mg and ^{44}Ca uptake was much lower than data reported for ^{15}N tracer studies. For example, Tietema et al. (1998) added soluble ^{15}N ($^{15}NH_4^{15}NO_3$) to throughfall and found on average 31.6 % of applied ^{15}N in aboveground biomass after only 12 months. Because allometric equations were fitted on a small number of sampled trees which did not cover the entire range of tree circumferences in the tracing plot, it is possible that tracer uptake was poorly estimated. However, tracer recovery (Fig. 10) after 2 years (102 ± 11 % of ^{26}Mg and 100 ± 18 % of ^{44}Ca) suggests that the estimation of tracer uptake is correct.

If we assume that the percentage of tracer uptake is representative of the proportion of atmospheric inputs directly taken up by trees, atmospheric inputs would only represent a 28 and 26 % of Mg and Ca uptake over 2 years. This suggests that the main Mg and Ca source for plant uptake is the soil. The slow transfer of Mg and Ca tracers in the soil as discussed below is in agreement with such a statement. However, this would contradict our main hypothesis that Mg and Ca atmospheric inputs are rapidly incorporated into the biological cycling of nutrients. Nevertheless, the tracing experiment results show that Mg and Ca cycling is very conservative. Indeed, the litter-layer, soil microbial biomass and the soil cationic exchange capacity proved to be very efficient to retain Mg and Ca inputs.

Conclusions

The in situ isotopic dilution technique using ^{26}Mg and ^{44}Ca at the ecosystem scale was proven to be an efficient method to assess Mg and Ca pool size change in the different ecosystem compartments. Decrease in

the soil exchangeable Mg pool was evidenced. Given high spatial variability, such a small change (-0.8 kg ha^{-1} year^{-1}) could not have been evidenced with conventional soil exchangeable pool comparisons. As soil exchangeable Mg pools decrease with time, concerns regarding the sustainability of such forests on base-poor soils are rising. Will Mg pools further decrease with time or will a compensation mechanism be triggered to buffer Mg depletion? We present evidence that conventional nutrient input–output budgets may largely over-estimate Ca depletion from the soil. To determine the sources of error in the Ca budgets specific experiments are required to test the different hypotheses: under-estimated inputs (atmospheric deposition, mineral weathering, and root nutrient uptake in deep soil layers) or over-estimation outputs (nutrient immobilization in tree biomass). These results confirm the conclusions drawn from the comparison of soil exchangeable pools in 1976 and 2001 (van der Heijden et al. 2013c): Mg has been continuously depleted from the soil while Ca pools appear to have remained constant. The future monitoring of ^{26}Mg and ^{44}Ca isotope dilution from Mg and Ca inputs to the ecosystem may enable us to better understand the dynamics of these nutrients in forest ecosystems.

Our isotopic dilution model may be used on a wider range of sites to estimate nutrient budgets and/or validate computed input–output budgets. Although, in this study, a very ^{26}Mg and ^{44}Ca enriched spike was used, it could be possible to set up experiments with less enriched material but using mass spectrometry instruments with higher precision in order to measure the isotopic dilution as proposed.

The results from the Mg and Ca tracing experiment show that the incorporation of Mg and Ca inputs to the nutrient cycles in the forest ecosystem is very slow even in a base-poor soil where nutrient cycling was expected to be fast to compensate for small Mg and Ca pools. However, Mg and Ca nutrient cycles were proven to be very conservative. Organic matter in the litter-layer and in the soil profile played an essential role in the incorporation of Mg and Ca inputs into the biogeochemical cycling of these nutrients within the forest ecosystem. The litter-layer, although very thin, very rapidly retained Mg and Ca inputs by ion exchange processes (cationic exchange capacity of litter). The vertical transfer of released tracers from the litter-layer was strongly influenced by preferential water flow which caused preferential leaching of Mg and Ca to deeper soil horizons. However, no tracer loss from the ecosystem was found. The dynamics of both nutrients differed: Mg was more mobile than Ca (faster release from the litter-layer and faster transfer to deep soil layers). We hypothesized that the cationic exchange capacity of the soil was dominated by organic CEC to explain such differences.

Tracing experiments using isotopically enriched material enable to gain considerable insight in nutrient cycling processes whether at the ecosystems scale or finer scales from the soil profile scale down to the soil particle scale. However, the limits of this kind of approach are due to the fact that the precision of isotope tracing experiments depends very largely on the precision of nutrient pool and flux measurements. Continuous effort to more precisely measure these pools and fluxes is necessary.

The results from the Mg and Ca tracing experiment also show the very important role of organic matter in Mg and Ca cycling in forest ecosystems. Organic matter, whether in the litter-layer or the soil, appears to be essential to soil fertility in forest ecosystems on base-poor soils, by rapidly retaining Mg and Ca inputs and thus limiting ecosystem losses for these nutrients. Climate change and silvicultural practices (such as whole tree harvesting or clear felling) may affect carbon cycling in soils and may thus strongly impact soil fertility in forest ecosystems on base poor soils where the soil total CEC is mainly dominated by organic CEC. By decreasing carbon pools in the soil profile, the soil total CEC may rapidly decrease followed by plant available base cations.

References

Achat DL, Bakker MR, Augusto L, Saur E, Dousseron L, Morel C (2009a) Evaluation of the phosphorus status of P-deficient podzols in temperate pine stands: combining isotopic dilution and extraction methods. Biogeochemistry 92(3): 183–200

Achat DL, Bakker MR, Morel C (2009b) Process-based assessment of phosphorus availability in a low phosphorus sorbing forest soil using isotopic dilution methods. Soil Sci Soc Am J 73(6):2131–2142

André JP, Pijarowski L (1977) Cation exchange properties of sphagnum peat: exchange between two cations and protons. J Soil Sci 28(4):573–584

Arocena JM, Velde B, Robertson SJ (2012) Weathering of biotite in the presence of *Arbuscular mycorrhizae* in selected agricultural crops. Appl Clay Sci 64:12–17

Augusto L, Zeller B, Midwood AJ, Swanston C, Dambrine E, Schneider A, Bosc A (2011) Two-year dynamics of foliage labelling in 8-year-old *Pinus pinaster* trees with (15)N, (26)Mg and (42)Ca-simulation of Ca transport in xylem using an upscaling approach. Ann For Sci 68(1):169–178

Baes AU, Bloom PR (1988) Exchange of alkaline earth cations in soil organic matter. Soil Sci 146(1):6–14

Bailey SW, Horsley SB, Long RP (2005) Thirty years of change in forest soils of the Allegheny plateau, Pennsylvania. Soil Sci Soc Am J 69(3):681–690

Bens O, Buczko U, Sieber S, Huttl RF (2006) Spatial variability of O layer thickness and humus forms under different pine beech-forest transformation stages in NE Germany. J Plant Nutr Soil Sci 169(1):5–15

Bolou-Bi EB, Poszwa A, Leyval C, Vigier N (2010) Experimental determination of magnesium isotope fractionation during higher plant growth. Geochim Cosmochim 74(9): 2523–2537

Bolou-Bi EB, Vigier N, Poszwa A, Boudot JP, Dambrine E (2012) Effects of biogeochemical processes on magnesium isotope variations in a forested catchment in the Vosges Mountains (France). Geochim Cosmochim 87:341–355

Bramley H, Hutson J, Tyerman SD (2003) Floodwater infiltration through root channels on a sodic clay floodplain and the influence of a local tree species *Eucalyptus largiflorens*. Plant Soil 253(1):275–286

Brethes A, Brun J, Jabiol B, Ponge J, Toutain F (1995) Classification of forest humus forms: a French proposal. Ann For Sci 52(6):535–546

Brookes PC, Powlson DS, Jenkinson DS (1982) Measurement of microbial biomass phosphorus in soil. Soil Biol Biochem 14(4):319–329

Brookes PC, Landman A, Pruden G, Jenkinson DS (1985) Chloroform fumigation and the release of soil-nitrogen—a rapid direct extraction method to measure microbial biomass nitrogen in soil. Soil Biol Biochem 17(6):837–842

Bukovac MJ, Wittwer SH (1957) Absorption and mobility of foliar applied nutrients. Plant Physiol 32(5):428–435

Calvaruso C, Turpault M-P, Frey-Klett P (2006) Root-associated bacteria contribute to mineral weathering and to mineral nutrition in trees: a budgeting analysis. Appl Environ Microbiol 72(2):1258–1266

Cenki-Tok B, Chabaux F, Lemarchand D, Schmitt A-D, Pierret M-C, Viville D, Bagard M-L, Stille P (2009) The impact of water–rock interaction and vegetation on calcium isotope fractionation in soil- and stream waters of a small, forested catchment (the Strengbach case). Geochim Cosmochim 73:2215–2228

Chishaki N, Yuda K, Inanaga S (2007) Differences in mobility of calcium applied to the above ground parts of broad bean plants (*Vicia faba* L.). Soil Sci Plant Nutr 53(3): 286–288

Cobert F, Schmitt AD, Bourgeade P, Labolle F, Badot PM, Chabaux F, Stille P (2011) Experimental identification of Ca isotopic fractionations in higher plants. Geochim Cosmochim 75(19):5467–5482

Cookson WR, Murphy DV (2004) Quantifying the contribution of dissolved organic matter to soil nitrogen cycling using 15N isotopic pool dilution. Soil Biol Biochem 36(12): 2097–2100

Curtin D, Selles F, Steppuhn H (1998) Estimating calcium–magnesium selectivity in smectitic soils from organic matter and texture. Soil Sci Soc Am J 62(5):1280–1285

DeSutter TM, Pierzynski GM, Baker LR (2006) Flow-through and batch methods for determining calcium-magnesium and magnesium–calcium selectivity. Soil Sci Soc Am J 70(2):550–554

Edwards CA, Bohlen PJ (1996) Biology and ecology of earthworms. Chapman and Hall Ltd., London

Ericsson K (2004) Bioenergy policy and market development in Finland and Sweden. Energy Policy 32:1707–1721

Evans LJ (1982) Cation exchange capacities and surface areas of humic gleysolic Ap horizons from southwestern Ontario. Can J Soil Sci 62(2):291–296

Farkaš J, Déjeant A, Novák M, Jacobsen SB (2011) Calcium isotope constraints on the uptake and sources of Ca^{2+}in a base-poor forest: a new concept of combining stable ($\delta^{44/42}Ca$) and radiogenic (εCa) signals. Geochim Cosmochim 75(22):7031–7046

Fletcher P, Sposito G, Levesque CS (1984) Sodium–calcium–magnesium exchange reactions on a montmorillonitic soil. 1. Binary exchange reactions. Soil Sci Soc Am J 48(5):1016–1021

Forbes GB, Perley A (1951) Estimation of total body sodium by isotopic dilution. I. Studies on young adults. J Clin Invest 30(6):558–565

Galy A, Yoffe O, Janney PE, Williams RW, Cloquet C, Alard O, Halicz L, Wadhwa M, Hutcheon ID, Ramon E, Carignan J (2003) Magnesium isotope heterogeneity of the isotopic standard SRM980 and new reference materials for magnesium-isotope-ratio measurements. J Anal At Spectrom 18(11):1352–1356

Gaston LA, Selim HM, Walthall PM (1993) Predicting cation transport in smectitic soils. Soil Sci Soc Am J 57(2):307–310

Granier A, Bréda N, Biron P, Villette S (1999) A lumped water balance model to evaluate duration and intensity of drought constraints in forest stands. Ecol Model 116:269–283

Hazlett PW, Curry JM, Weldon TP (2011) Assessing decadal change in mineral soil cation chemistry at the Turkey lakes watershed. Soil Sci Soc Am J 75(1):287–305

Helling CS, Chesters G, Corey RB (1964) Contribution of organic matter and clay to soil cation-exchange capacity as affected by the pH of the saturating solution. Soil Sci Soc Am J 28(4):517–520

Hindshaw R, Reynolds B, Wiederhold J, Kiczka M, Kretzschmar R, Bourdon B (2012) Calcium isotope fractionation in alpine plants. Biogeochemistry 112(1–3):373–388

Hoefs J (2009) Stable isotope geochemistry, 6th edn. Springer, Germany

Holmden C, Bélanger N (2010) Ca isotope cycling in a forested ecosystem. Geochim Cosmochim 74:995–1015

Johnson DW (1995) Temporal patterns in beech forest soil solutions—field and model results compared. Soil Sci Soc Am J 59(6):1732–1740

Johnson CE (2002) Cation exchange properties of acid forest soils of the northeastern USA. Eur J Soil Sci 53(2):271–282

Johnson DW, Todd DE (1998) Harvesting effects on long-term changes in nutrient pools of mixed oak forest. Soil Sci Soc Am J 62(6):1725–1735

Johnson DW, West DC, Todd DE, Mann LK (1982) Effects of sawlog vs. whole-tree harvesting on the nitrogen,

phosphorus, potassium, and calcium budgets of an upland mixed oak forest. Soil Sci Soc Am J 46(6):1304–1309
Johnson DW, Sogn T, kvindesland S (2000) The nutrient cycling model: lessons learned. Forest Ecol Manag 138:91–106
Johnson DW, Todd DE Jr, Trettin CF, Mulholland PJ (2008) Decadal changes in potassium, calcium, and magnesium in a deciduous forest soil. Soil Sci Soc Am J 72(6):1795–1805
Jonard M, Legout A, Nicolas M, Dambrine E, Nys C, Ulrich E, van der Perre R, Ponette Q (2012) Deterioration of Norway spruce vitality despite a sharp decline in acid deposition: a long-term integrated perspective. Glob Change Biol 18(2):711–725
Klaminder J, Lucas RW, Futter MN, Bishop KH, Kohler SJ, Egnell G, Laudon H (2011) Silicate mineral weathering rate estimates: are they precise enough to be useful when predicting the recovery of nutrient pools after harvesting? For Ecol Manag 261(1):1–9
Krishnamoorthy C, Overstreet R (1950) An experimental evaluation of ion-exchange relationships. Soil Sci 69(1):41–54
Kuhn AJ, Schroder WH, Bauch J (2000) The kinetics of calcium and magnesium entry into mycorrhizal spruce roots. Planta 210(3):488–496
Legout A (2008) Cycles Biogéochimiques et bilans de fertilité minérale en hêtraies de plaine. Agroparistech-Engref, Nancy, p 281
Legout A, Walter C, Nys C (2008) Spatial variability of nutrient stocks in the humus and soils of a forest massif (Fougeres, France). Ann For Sci 65(1):108
Lequy E, Conil S, Turpault MP (2012) Impacts of Aeolian dust deposition on European forest sustainability: a review. For Ecol Manag 267:240–252
Lorenz N, Verdell K, Ramsier C, Dick RP (2010) A rapid assay to estimate soil microbial biomass potassium in agricultural soils. Soil Sci Soc Am J 74(2):512–516
Mansell RS, Bloom SA, Selim HM, Rhue RD (1988) Simulated transport of multiple cations in soil using variable selectivity coefficients. Soil Sci Soc Am J 52(6):1533–1540
Mansell RS, Bond WJ, Bloom SA (1993) Simulating cation transport during water flow in soil—2. Approaches. Soil Sci Soc Am J 57(1):3–9
Mareschal L (2008) Effet des substitutions d'essences forestières sur l'évolution des sols et de leur minéralogie : bilan après 28 ans dans le site expérimental de Breuil (Morvan). Université Henri Poincaré, Ressources Procédés Produits Environnement, Nancy, p 328
Marschner H (1995) Mineral nutrition of higher plants. Academic, London
Martinez-Meza E, Whitford WG (1996) Stemflow, throughfall and channelization of stemflow by roots in three Chihuahuan desert shrubs. J Arid Environ 32(3):271–287
Midwood AJ, Proe MF, Harthill JJ (2000) Use and analysis by thermal ionisation mass spectrometry of Mg-26 and K-41 to assess mineral uptake in Scots pine (*Pinus sylvestris* L.). Analyst 125(3):487–492
Momii K, Hiroshiro Y, Jinno K, Berndtsson R (1997) Reactive solute transport with a variable selectivity coefficient in an undisturbed soil column. Soil Sci Soc Am J 61(6):1539–1546
Moukoumi J (2006) Effet des essences forestières sur la biodégradation des matières organiques: impacts sur la dynamique et le cycle du carbone, de l'azote et des éléments minéraux. Université Henri Poincaré, Nancy, p 255
Oorts K, Vanlauwe B, Merckx R (2003) Cation exchange capacities of soil organic matter fractions in a Ferric Lixisol with different organic matter inputs. Agric Ecosyst Environ 100(2–3):161–171
Palviainen M, Finér L, Kurka A-M, Mannerkoski H, Piirainen S, Starr M (2004) Release of potassium, calcium, iron and aluminium from Norway spruce, Scots pine and silver birch logging residues. Plant Soil 269:123–136
Paul JL, Tanji KK, Anderson WD (1966) Estimating soil and saturation extract composition by a computer method. Soil Sci Soc Am J 30(1):15–17
Ponette Q, Dufey JE, Weissen F (1997) Downward movement of dolomite, kieserite or a mixture of CaCO3 and kieserite through the upper layers of an acid forest soil. Water Air Soil Pollut 95(1–4):353–379
Pratt PF (1961) Effect of pH on the cation-exchange capacity of surface soils. Soil Sci Soc Am J 25(2):96–98
Puech J (2009) Mise en valeur de la forêt française et développement de la filière bois. Federal Office for the Environment, Bern, p 75
Ranger J, Andreux F, Bienaimé S, Berthelin J, Bonnaud P, Boudot JP, Bréchet C, Buée M, Calmet J, Chaussod R, Gelhaye D, Gelhaye L, Gérard F, Jaffrain J, Lejon D, Le Tacon F, Lévêque J, Maurice J, Merlet D, Moukoumi J, Munier-Lamy C, Nourrisson G, Pollier B, Ranjard L, Simonsson M, Turpault MP, Vairelles D, Zeller B (2004) Effet des substitutions d'essence sur le fonctionnement organo-minéral de l'écosystème forestier, sur les communautés microbiennes et sur la diversité des communautés fongiques mycorhiziennes et saprophytes (cas du dispositif de Breuil—Morvan), Rapport final contrat INRA-GIP Ecofor 2001–2024, no. INRA 1502A. INRA Biogéochimie des Ecosystèmes Forestiers (UR 1138). Institut national de la recherche agronomique (INRA), Champenoux
Ross DS, Bartlett RJ, Magdoff FR (1991) Exchangeable cations and the pH-independent distribution of cation exchange capacities in Spodosols of a forested watershed. Plant–soil interactions at Low pH. Springer, Netherlands, pp 81–92
Russell WA, Papanastassiou DA, Tombrello TA (1978) Ca isotope fractionation on earth and other solar-system materials. Geochim Cosmochim 42(8):1075–1090
Saggar S, Bettany JR, Stewart JWB (1981) Measurement of microbial sulfur in soil. Soil Biol Biochem 13(6):493–498
Salmon RC (1964) Cation exchange reactions. J Soil Sci 15(2):273–283
Suarez DL, Zahow MF (1989) Calcium-magnesium exchange selectivity of Wyoming montmorillonite in chloride, sulphate and perchlorate solutions. Soil Sci Soc Am J 53(1):52–57
Sentenac H, Grignon C (1981) A model for predicting ionic equilibrium concentrations in cell-walls. Plant Physiol 68(2):415–419
Sparling GP, West AW (1988) A direct extrcation method to estimate soil microbial-C—calibration in situ using microbial respiration and 14C leabeled cells. Soil Biol Biochem 20(3):337–343
Sposito G, Fletcher P (1985) Sodium calcium magnesium exchange-reactions on a montmorillonitic soil. 3.

Calcium–magnesium exchange selectivity. Soil Sci Soc Am J 49(5):1160–1163

Sposito G, Holtzclaw KM, Jouany C, Charlet L (1983) Cation selectivity in sodium–calcium, sodium–magnesium, and calcium–magnesium exchange on Wyoming bentonite at 298-K. Soil Sci Soc Am J 47(5):917–921

Staelens J, Houle D, De Schrijver A, Neirynck J, Verheyen K (2008) Calculating dry deposition and canopy exchange with the canopy Budget model: review of assumptions and application to two deciduous forests. Water Air Soil Pollut 191:149–169

Stroud JL, Khan MA, Norton GJ, Islam MR, Dasgupta T, Zhu Y-G, Price AH, Meharg AA, McGrath SP, Zhao F-J (2011) Assessing the labile arsenic pool in contaminated paddy soils by isotopic dilution techniques and simple extractions. Environ Sci Technol 45(10):4262–4269

Sverdrup H, Warfvinge (1988) Weathering of primary silicate minerals in the natural soil environment in relation to a chemical weathering model. Water Air Soil Pollut 38:387–408

Thompson ML, Zhang H, Kazemi M, Sandor JA (1989) Contribution of organic-matter to cation exchange capacity and specific surface area of fractionated soil materials. Soil Sci 148(4):250–257

Tietema A, Emmett BA, Gundersen P, Kjonaas OJ, Koopmans CJ (1998) The fate of N-15-labelled nitrogen deposition in coniferous ecosystems. For Ecol Manag 101(1–3):19–27

Turpault MP, Bonnaud P, Fichter J, Ranger J, Dambrine E (1996) Distribution of cation exchange capacity between organic matter and mineral fractions in acid forest soils (Vosges mountains, France). Eur J Soil Sci 47(4):545–556

Turpault MP, Nys C, Calvaruso C (2009) Rhizosphere impact on the dissolution of test minerals in a forest ecosystem. Geoderma 153(1–2):147–154

Udo EJ (1978) Thermodynamics of potassium-calcium and magnesium-calcium exchange reactions on a kaolinitic soil clay. Soil Sci Soc Am J 42(4):556–560

Ulrich B (1983) Interaction of forest canopies with atmospheric constituents: SO_2, alkali and earth alkali cations and chloride. In: Ulrich B, Pankrath J (eds) Effects of accumulation of air pollutants in forest ecosystems. D Reidel, Boston, pp 33–45

van der Heijden G, Legout A, Nicolas M, Ulrich E, Johnson DW, Dambrine E (2011) Long-term sustainability of forest ecosystems on sandstone in the Vosges Mountains (France) facing atmospheric deposition and silvicultural change. For Ecol Manag 261(3):730–740

van der Heijden G, Legout A, Midwood A, Craig C-A, Pollier B, Ranger J, Dambrine E (2013a) Mg and Ca root uptake and vertical transfer in soils assessed by an in situ ecosystem-scale multi-isotopic (^{26}Mg and ^{44}Ca) tracing experiment in a beech stand (Breuil-Chenue, France). Plant Soil 369(1–2):33–45

van der Heijden G, Legout A, Pollier B, Bréchet C, Ranger J, Dambrine E (2013b) Tracing and modeling preferential flow in a forest soil—potential impact on nutrient leaching. Geoderma 195–196:12–22

van der Heijden G, Legout A, Pollier B, Mareschal L, Turpault MP, Ranger J, Dambrine E (2013c) Assessing Mg and Ca depletion from broadleaf forest soils and potential causes—a case study in the Morvan Mountains. For Ecol Manag 293:65–78

Vance ED, Brookes PC, Jenkinson DS (1987) An extraction method for measuring soil microbial biomass-C. Soil Biol Biochem 19(6):703–707

Verrecchia E, Braissant O, Cailleau G (2006) The oxalate-carbonate pathway in soil carbon storage: the role of fungi and axalotrophic bacteria. Fungi Biochem Cycles 12:289–310

von Hevesy G, Hofer E (1934) Die verweilzeit des wassers im menschilchen körper, untersucht mit hilfe von "schwerem" wasser als indicator. Klinische Wochenschrift 13:1524

Weatherall A, Proe MF, Craig J, Cameron AD, McKay HM, Midwood AJ (2006) Tracing N, K, Mg and Ca released from decomposing biomass to new tree growth. Part I: a model system simulating harvest residue decomposition on conventionally harvested clearfell sites. Biomass Bioenerg 30(12):1053–1059

Wiegand BA, Chadwick OA, Vitousek PM, Wooden JL (2005) Ca cycling and isotopic fluxes in forested ecosystems in Hawai. Geophys Res Lett 32(11):L11404

Wilding LP, Rutledge EM (1966) Cation-exchange capacity as a function of organic matter, total clay, and various clay fractions in a soil toposequence. Soil Sci Soc Am J 30(6):782–785

Willison TW, Baker JC, Murphy DV, Goulding KWT (1998) Comparison of a wet and dry 15N isotopic dilution technique as a short-term nitrification assay. Soil Biol Biochem 30(5):661–663

Wittwer SH, Teubner FG (1959) Foliar absorption of mineral nutrients. Ann Rev Plant Physiol 10:13–30

Wright WR, Foss JE (1972) Contributions of clay and organic matter to the cation exchange capacity of Maryland soils. Soil Sci Soc Am J 36(1):115–118

Yanai RD, Blum JD, Hamburg SP, Arthur MA, Nezat CA, Siccama TG (2005) New insights into calcium depletion in northeastern forests. J For 103(1):14–20

Yuan TL, Gammo N, Leighty RG (1967) Relative contribution of organic and clay fractions to cation-exchange capacity of sandy soils from several soil groups. Soil Sci 104(2):123–128